

Supporting information for

Selective synthesis and structural transformation between ring-in-ring architecture and abnormal trefoil knot

Li-Long Dang,^a Xiang Gao,^a Yue-Jian Lin,^a and Guo-Xin Jin^{*ab}

a. Shanghai Key Laboratory of Molecular Catalysis and Innovative Materials, State Key Laboratory of Molecular Engineering of Polymers, Department of Chemistry, Fudan University, Shanghai 200438, P. R. China

b. State Key Laboratory of Organometallic Chemistry, Shanghai Institute of Organic Chemistry, Chinese Academy of Sciences, Shanghai 200032, P. R. China.

*E-mail: gxjin@fudan.edu.cn.

Contents

1. General considerations	2
2. Synthesis of complexes L, complex 1, 1', 2, 2', 2-pyrene, 3, 3', 4 and 5	2
3. Single-crystal X-ray structure of 3', 3, 4 and 5	5
4. NMR spectra	8
5. ESI-MS spectra	22
6. X-ray crystallography details	25
7. References	32

1. General considerations

All reagents and solvents were purchased from commercial sources and used as supplied unless otherwise mentioned. The starting materials $[\text{Cp}^*\text{RhCl}_2]_2$ and $[\text{Cp}^*\text{IrCl}_2]_2$ ($\text{Cp}^* = \eta^5\text{-pentamethylcyclopentadienyl}$)^[1], BiBzIm (BiBzIm = 2,2'-bisbenzimidazole)^[2] TmBiBzIm (TmBiBzIm = 5,5',6,6'-tetramethyl-1H,1'H-2,2'-bibenzo[d]imidazole)^[3] $[\text{Cp}^*_2\text{Rh}_2(\text{BiBzIm})(\text{OTf})_2]$ (**E1**)^[2], $[\text{Cp}^*_2\text{Ir}_2(\text{BiBzIm})(\text{OTf})_2]$ (**E1'**)^[2], $[\text{Cp}^*_2\text{Rh}_2(\text{TmBiBzIm})(\text{OTf})_2]$ (**E2**)^[5], $[\text{Cp}^*_2\text{Rh}_2(\mu\text{-}\eta^4\text{-C}_2\text{O}_4)(\text{OTf})_2]$ (**E4**)^[4], $[\text{Cp}^*_2\text{Rh}_2(\mu\text{-CA})]\text{Cl}_2$ ^[6] (**E5**), and ligand **L**^[7] were prepared by literature methods. NMR spectra were recorded on Bruker AVANCE I 400 spectrometers at room temperature and referenced to the residual protonated solvent. Proton chemical shifts are reported relative to the solvent residual peak (δ H = 3.31 (CD₃OD), 2.50 (DMSO-D6), 1.94 (CD₃CN), 2.75, 2.92 (DMF)) and δ C = 49.00 (CD₃OD), 29.76, 34.89 (DMF)). Coupling constants are expressed in Hertz. Elemental analyses were performed on an Elementar Vario EL III analyzer. ESI-MS spectra were recorded on a Micro TOF II mass spectrometer.

2. Synthesis of ligand L, complex 1, 1', 2, 2', 2-pyrene, 3, 3' 4, and 5

Synthesis of N, N'-bis(4-pyridylmethyl)-diphthalic diimide (L): A mixture of diphthalic dianhydride (3.1 g, 10 mmol) and 4-aminomethyl-pyridine (2.2 g, 21 mmol) in DMF (40 mL) was heated to reflux with stirring for 5 h. On cooling of the sample, the yellow solution was filtered, and the off-white crude solid was collected and washed with cold DMF. A white powder was obtained by recrystallization of the solid from DMF. Yield: 82%. Anal. cald. for C₂₈H₁₈O₄N₄: C, 70.88; H, 3.82; N, 11.81. Found: C, 70.96; H, 3.78; N, 11.86%. ¹H NMR (ppm, DMSO-d₆) δ : 8.53 (d, J = 4 Hz, 4H), 8.36 (s, 2H), 8.33 (d, J = 8 Hz, 2H), 8.05 (d, J = 8 Hz, 2H), 7.35 (d, J = 4 Hz, 4H), 4.86 (s, 4H).

Preparation of complex 1

AgOTf (123.2 mg, 0.48 mmol) was added to a solution of $[\text{Cp}^*\text{RhCl}_2]_2$ (74.4 mg, 0.12 mmol) in a CH₃CN (8 mL) at room temperature. The reaction mixture was stirred in the dark for 24 h and then filtered. BiBzIm (28.0 mg, 0.12mmol) was added to the filtrate. The mixture was stirred at room temperature for 12 h to give a yellow solution. **L** (56.88 mg, 0.12 mmol) was then added. The mixture was stirred at room temperature for another 12 h to give a yellow solution. Upon the addition of diethyl ether, a yellow solid was precipitated and collected. The product was recrystallized from a CH₃OH/diethyl ether mixture to afford block-shaped crystals (**1**). 156.30 mg, yield 88%. Anal. Calcd for C₁₂₈H₁₁₂N₁₆O₂₀F₁₂S₄Rh₄ (M=2960.32): C, 51.90; H, 3.81; N, 7.57. Found: C, 51.95; H, 3.83, N, 7.55. ¹ H NMR (400 MHz, CD₃CN, ppm, with respect to Cp*Rh): δ =8.28 (d, J=8Hz, 8H, pyridyl- α H), δ = 7.97 (s, 4H, phenyl-H), δ = 7.95 (d, J=4Hz, 8H, BiBzIm-H), δ = 7.89 (s, 4H, phenyl-H), δ = 7.70 (d, J=8Hz, 4H, phenyl-H), δ =7.46 (q, J=4Hz, 8H, BiBzIm-H), δ =7.09 (d, J=8Hz, 8H, pyridyl- β H), δ = 4.35 (s, 8H, CH₂), δ =1.68 (s, 60H, Cp*-H). ¹³C{¹H} (101 MHz, CD₃OD, ppm): δ =10.18 (Cp*), 40.47, 98.05, 98.13, 117.19, 118.30, 122.91, 132.25, 134.19, 144.27, 149.71, 153.64, 157.09, 167.64, 167.73.

Preparation of complex 1'

AgOTf (123.2 mg, 0.48 mmol) was added to a solution of $[\text{Cp}^*\text{IrCl}_2]_2$ (96.00 mg, 0.12 mmol) in CH₃CN (8 mL) at room temperature. The reaction mixture was stirred in the dark for 24 h and then filtered. BiBzIm (28.0 mg, 0.12mmol) was added to the filtrate. The mixture was stirred at room temperature for 12 h to give a yellow solution. **L** (56.88 mg, 0.12 mmol) was then added. The mixture was stirred at room temperature for another 12 h to give a yellow solution. Upon the addition of diethyl ether, a yellow solid was precipitated and collected. The product was recrystallized from a CH₃OH/diethyl ether mixture to afford block-shaped crystals (**1'**). 142.25mg, yield: 83%. Anal. Calcd for C₁₂₈H₁₁₂N₁₆O₂₀F₁₂S₄Ir₄ (M=3320.54): C, 46.31; H, 3.40; N, 6.75. Found: C, 46.35; H, 3.43, N, 6.71.

Preparation of complex 2

AgOTf (123.2 mg, 0.48 mmol) was added to a solution of [Cp*RhCl₂]₂ (74.4 mg, 0.12 mmol) in CH₃OH (8 mL) at room temperature. The reaction mixture was stirred in the dark for 24 h and then filtered. BiBzIm (28.0 mg, 0.12 mmol) was added to the filtrate. The mixture was stirred at room temperature for 12 h to give a yellow solution. **L** (56.88 mg, 0.12 mmol) was then added. The mixture was stirred at room temperature for another 12 h to give a yellow solution. The solvent was concentrated to about 7 mL. Then, a 1:1 mixture of methanol and isopropyl ether was added into the mother solution gradually until the yellow solution became a colorless liquid. After that, the equivalent isopropyl ether was added. Block-shaped single crystals suitable for X-ray diffraction were obtained (**2**) after 3 days. 136.69 mg, yield: 82%. Anal. Calcd for C₂₅₆H₂₂₄N₃₂Rh₈O₄₀S₈F₂₄ (M=5556.55): C, 55.30; H, 4.06; N, 1.51. Found: C, 55.34; H, 4.03; N, 1.54. IR (KBr disk, cm⁻¹): ν = 1772, 1717, 1617, 1450, 1427, 1391, 1356, 1258, 1225, 1162, 1115, 1066, 1032, 946, 775, 748, 639, 574, 518, 495.

Preparation of complex 2'

AgOTf (123.2 mg, 0.48 mmol) was added to a solution of [Cp*IrCl₂]₂ (96.00 mg, 0.12 mmol) in CH₃OH (16 mL) at room temperature. The reaction mixture was stirred in the dark for 24 h and then filtered. BiBzIm (28.0 mg, 0.12 mmol) was added to the filtrate. The mixture was stirred at room temperature for 12 h to give a yellow solution. **L** (56.88 mg, 0.12 mmol) was then added. The mixture was stirred at room temperature for another 12 h to give a yellow solution. The solvent was concentrated to about 7 mL. Then, a 1:1 mixture of methanol and isopropyl ether was added into the mother solution gradually until the yellow solution became a colorless liquid. After that, the equivalent isopropyl ether was added. Block-shaped single crystals suitable for X-ray diffraction were obtained after 3 days (**2'**). 163.83 mg, yield: 87%.

Preparation of complex 2-pyrene

Guest molecule pyrene (36.4 mg, 0.18 mmol) were added to the self-assembly process of **E1** (26.20 mg, 0.03 mmol) and **L** (14.22 mg, 0.03 mmol) in a methanol solution (8 mL). The mixture was stirred at room temperature for 24 h and then filtered. The solvent was concentrated to about 4 mL. Upon the addition of diethyl ether, a dark-yellow solid was precipitated and collected. After recrystallization, a dark-yellow crystalline solid was obtained in quantitative yield. Anal. calcd for C₂₅₆H₂₂₄N₃₂Rh₈O₄₀S₈F₂₄ (pyrene)_n

Preparation of complex 3

AgOTf (123.2 mg, 0.48 mmol) was added to a solution of [Cp*RhCl₂]₂ (74.4 mg, 0.12 mmol) in CH₃OH (16 mL) at room temperature. The reaction mixture was stirred in the dark for 24 h and then filtered. BiBzIm (28.0 mg, 0.12 mmol) was added to the filtrate. The mixture was stirred at room temperature for 12 h to give a yellow solution. **L** (56.88 mg, 0.12 mmol) was then added. The mixture was stirred at room temperature for another 12 h to give a yellow solution. Subsequently, AgOTf (20.53 mg, 0.08 mmol) and BiBzIm (9.33 mg, 0.04 mmol) was added into the above solution. The mixture was stirred at room temperature for final 12 h. The solvent was concentrated to about 7 mL. Upon the addition of diethyl ether, a yellow solid was precipitated and collected. The product was recrystallized from a CH₃OH/diethyl ether mixture to afford block-shaped crystals (**3**). 173.95 mg, yield: 89 %. Anal. calcd (%) for C₂₀₆H₁₇₆N₂₈O₃₀Ag₂Rh₆S₆F₁₈ (M=4886.36): C 50.58, H 3.63, N 8.02. Found: C 50.54, H 3.61, N 8.06. ¹H NMR (400 MHz, CD₃OD, ppm): δ 8.80-8.77 (m, **pyridyl-H**, 8H), δ 8.43 (d, J = 8.0 Hz, **BiBzIm-H**, 2H), 8.20 (d, J = 8.0 Hz, **BiBzIm-H**, 2H), 8.12 (d, J = 7.6 Hz, **BiBzIm-H**, 2H), 8.07 (d, J = 8.4 Hz, **BiBzIm-H**, 2H), 7.93 (d, J = 8.4 Hz, **BiBzIm-H**, 2H), 7.86 (s, **L-PDM-H**, 2H), 7.84-7.80 (m, **BiBzIm-H**, 4H and **pyridyl-H**, 4H), 7.70-7.59 (m, **BiBzIm-H**, 8H and **L-PDM-H**, 2H), 7.51 (t, J = 7.6 Hz, **BiBzIm-H**, 2H), 7.37-7.33 (m, **pyridyl-H**, 8H), 7.19 (d, J = 8.0 Hz, **BiBzIm-H**, 2H), 7.03 (d, J = 7.6 Hz, **BiBzIm-H**, 2H), 6.87 (s, **pyridyl-H**, 4H), 6.75 (s, **L-PDM-H**, 2H), 6.09 (s, **BiBzIm-H**, 4H), 5.95 (s, **L-PDM-H**,

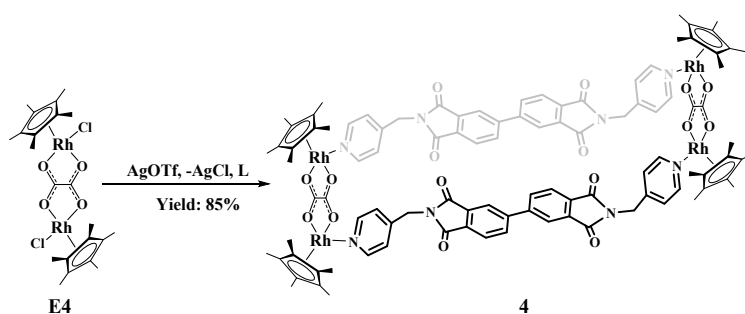
2H), 5.17 (d, J = 16.8 Hz, $-\text{CH}_2$, 2H), 5.08 (d, J = 5.2 Hz, **L-PDM-H**, 2H), 5.06 (d, J = 5.2 Hz, **L-PDM-H**, 2H), 4.59 (d, J = 7.6 Hz, **L-PDM-H**, 2H), 4.40 (d, J = 14.8 Hz, $-\text{CH}_2$, 2H), 4.34 (d, J = 18.4 Hz, $-\text{CH}_2$, 2H), 4.17 (d, J = 8.0 Hz, $-\text{CH}_2$, 2H), 4.15 (d, J = 8.4 Hz, **L-PDM-H**, 2H), 3.84 (d, J = 14.4 Hz, $-\text{CH}_2$, 2H), 3.81 (d, J = 7.2 Hz, **L-PDM-H**, 2H), $\delta=1.79$ (s, Cp*-H, 30H), $\delta=1.66$ (s, Cp*-H, 30H), $\delta=1.50$ (s, Cp*-H, 30H). $^{13}\text{C}\{^1\text{H}\}$ (101 MHz, CD_3OD , ppm): $\delta=10.05$ (Cp*), 10.01 (Cp*), 9.67 (Cp*), 31.65, 36.94, 40.85, 98.41, 98.47, 98.68, 98.75, 98.81, 98.88, 117.21, 117.58, 119.57, 123.24, 123.47, 124.01, 124.50, 124.57, 124.95, 125.47, 125.73, 125.79, 126.59, 129.62, 132.45, 132.59, 132.78, 135.05, 140.61, 145.02, 145.20, 145.26, 145.70, 149.79, 151.47, 154.82, 155.25, 164.86, 166.87, 167.01, 167.77. IR (KBr disk, cm^{-1}): $\nu = 1772, 1718, 1616, 1653, 1568, 1451, 1427, 1385, 1355, 1283, 1252, 1225, 1163, 1031, 974, 911, 845, 751, 639, 575, 518, 495$.

Preparation of complex 3'

The synthesis of **3'** was carried out similarly to that of **3** with the use of TmBiBzIm (34.8 mg, 0.12 mmol) instead of BiBzIm (28.0 mg, 0.12 mmol). After extraction with diethyl ether, the yellow product was separated by centrifugation and dried under vacuum. 183.98 mg, yield: 90%. Anal. calcd (%) for $\text{C}_{222}\text{H}_{208}\text{N}_{28}\text{O}_{30}\text{Ag}_2\text{Rh}_6\text{F}_{18}\text{S}_6$ (M=5110.61): C 52.12, H 4.10, N 7.67. Found: C 52.15, H 4.14, N 7.64.

Preparation of complex 4

AgOTf (15.4 mg, 0.06 mmol) was added to a solution of $[\text{Cp}^*_2\text{Rh}_2(\mu\text{-}\eta^4\text{-C}_2\text{O}_4)]\text{Cl}_2$ (0.03 mmol, 19.12 mg) in CH_3OH (5 mL) at room temperature. The reaction mixture was stirred in the dark for 24 h and then filtered. **L** (14.22 mg, 0.03 mmol) was added to the filtrate. The mixture was stirred at room temperature for 24 h to give a yellow solution. The solvent was concentrated to about 2 mL. Upon the addition of diethyl ether, a yellow solid precipitated and was collected. The product was recrystallized from a CH_3OH /diethyl ether mixture to afford a yellow solid. 34.07 mg, yield 85%. X-ray quality crystals of **4** were obtained by slow diffusion of diethyl ether into a methanol solution of **4** at room temperature. Anal. calcd (%) for $\text{C}_{104}\text{H}_{96}\text{N}_8\text{Rh}_4\text{S}_4\text{O}_{28}\text{F}_{12}$ (M=2672.12): C 46.72, H 3.62, N 4.19. Found: C 46.75, H 3.64, N 4.15. IR (KBr disk, cm^{-1}): $\nu = 1772, 1717, 1619, 1427, 1391, 1363, 1273, 1224, 1156, 1113, 1066, 1032, 947, 867, 796, 748, 637, 573, 518, 468$. ^1H NMR (400 MHz, CD_3OD , ppm): $\delta=8.152$ (d, J=5.6 Hz, 8H, pyridyl- αH), $\delta=7.986$ (d, J=7.6 Hz, 4H phenyl-H), $\delta=7.930$ (s, 4H, phenyl-H), $\delta=7.798$ (d, J=7.6 Hz, 4H, phenyl-H), $\delta=7.503$ (d, J=5.6 Hz, 8H, pyridyl- βH), $\delta=4.965$ (s, 8H, CH_2), $\delta=1.642$ (s, 60H, Cp*-H). $^{13}\text{C}\{^1\text{H}\}$ (101 MHz, CD_3OD , ppm): $\delta=8.46$ (Cp*), 39.72, 41.20, 97.00, 123.03, 125.16, 125.80, 132.74, 134.45, 145.50, 151.56, 152.06, 168.62, 168.75, 171.22.

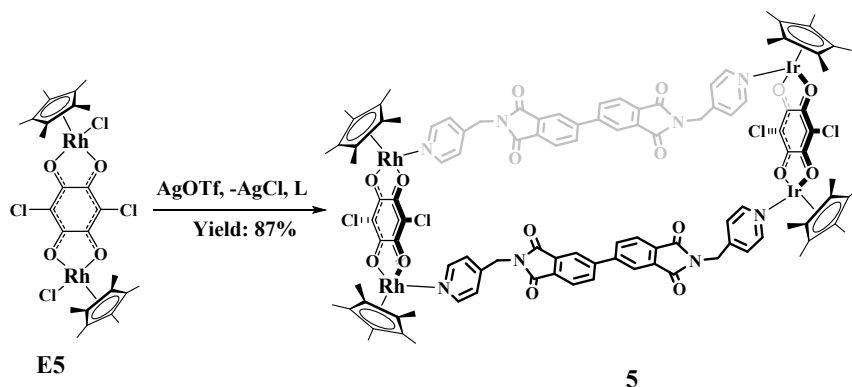


Scheme S1. Self-assembly of tetranuclear metallarectangle **4**.

Preparation of complex 5

AgOTf (15.4 mg, 0.06 mmol) was added to a solution of $[\text{Cp}^*_2\text{Rh}_2(\mu\text{-CA})]\text{Cl}_2$ (0.03 mmol, 23.00 mg) in CH_3OH (5 mL) at room temperature. The reaction mixture was stirred in the dark for 24 h and then filtered. **L** (14.22 mg, 0.03 mmol) was added to the filtrate. The mixture was stirred at room temperature for 24 h to give a yellow solution. The solvent was concentrated to about 2 mL. Upon the addition of diethyl ether, a yellow solid precipitated and was collected. The product was recrystallized from a CH_3OH /diethyl ether mixture to afford a

yellow solid. 38.00 mg, yield: 87%. X-ray quality crystals of **5** were obtained by slow diffusion of diethyl ether into a methanol solution of **5** at room temperature. Anal. calcd (%) for $C_{112}H_{100}N_8O_{28}Rh_4Cl_4S_4F_{12}$ ($M=2768.12$): C 48.57, H 3.49, N 4.05. Found: C 48.54, H 3.46, N 4.08. IR (KBr disk, cm^{-1}): $\nu = 1772, 1716, 1618, 1524, 1427, 1390, 1361, 1261, 1225, 1161, 1117, 1065, 1032, 950, 843, 754, 639, 573, 518, 490$. 1H NMR (400 MHz, CD_3OD , ppm): $\delta=8.304$ (d, $J=6.0$ Hz, 8H, pyridyl- α H), $\delta= 8.133$ (d, $J=8.0$ Hz, 4H phenyl-H), $\delta= 8.100$ (s, 4H, phenyl-H), $\delta= 7.851$ (d, $J=7.6$ Hz, 4H, phenyl-H), $\delta=7.534$ (d, $J=6.0$ Hz, 8H, pyridyl- β H), $\delta= 4.692$ (s, 8H, CH_2), $\delta=1.687$ (s, 60H, Cp*-H). $^{13}C\{^1H\}$ (101 MHz, CD_3OD , ppm): $\delta=8.71$ (Cp*), 41.01, 97.75, 97.83, 107.17, 123.00, 125.32, 127.29, 132.86, 134.17, 145.46, 151.32, 152.52, 168.37, 168.41, 177.96.



Scheme S2. Self-assembly of tetranuclear metallarectangle **5**.

3. Single-crystal X-ray structure of **1**, **3'**, **3** and **5**

3.1 Single-crystal X-ray structure of **3'**

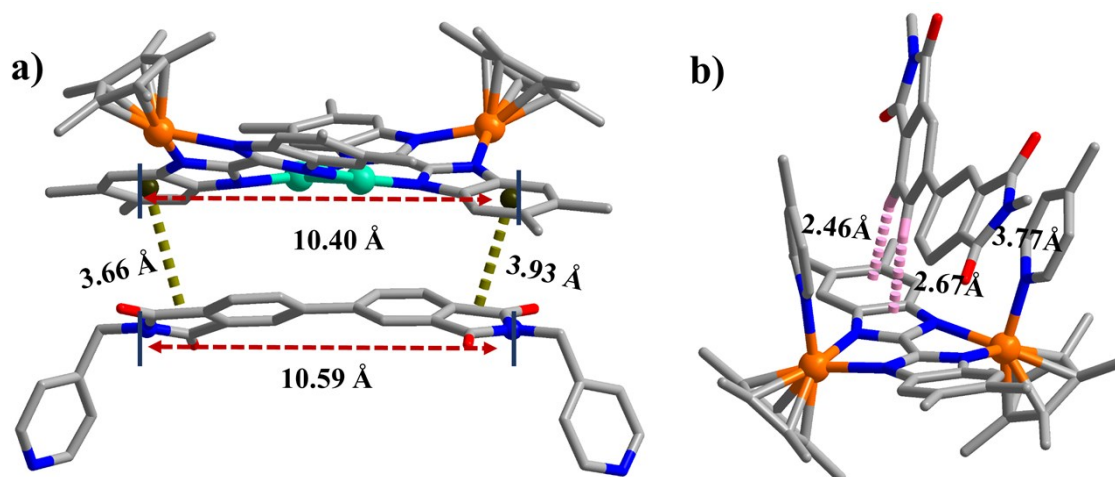


Fig. S1. Partial presentation of single-crystal X-ray structure of **3'**, π - π stacking interactions between the phthalic diimide moieties of **L** and benzene rings of the TmBiBzIm moieties of **E3'**; (a) C-H $\cdots\pi$ interactions between protons of benzene rings of **L** and TmBiBzIm moiety. (b) Counteranions and other hydrogen atoms are omitted for clarity (N, blue; O, red; C, gray; Rh, orange; H, rose).

3.2 Single-crystal X-ray structure of 3

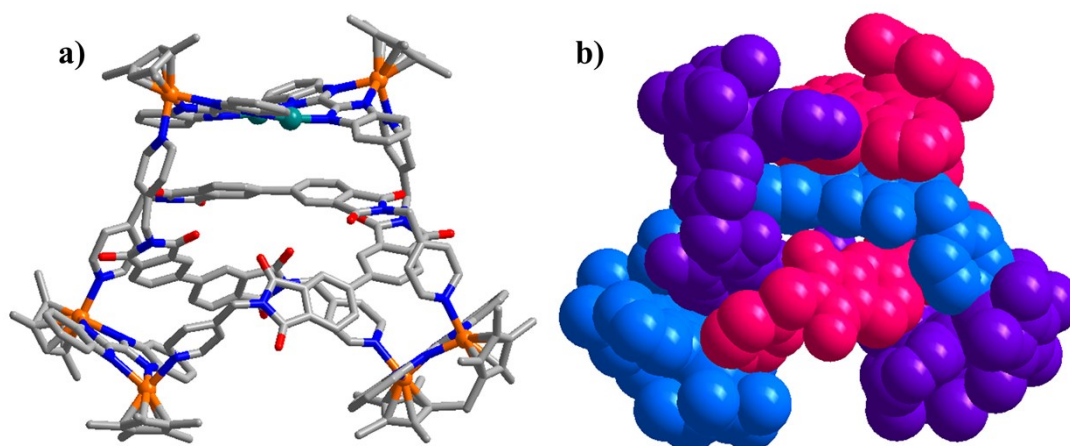


Fig. S2. a) Single-crystal X-ray structure of **3**; b) View of asymmetrical trefoil knot **3** in space-filling mode; Counteranions and hydrogen atoms are omitted for clarity (N, blue; O, red; C, gray; Rh, orange)

3.3 Single-crystal X-ray structure of 4

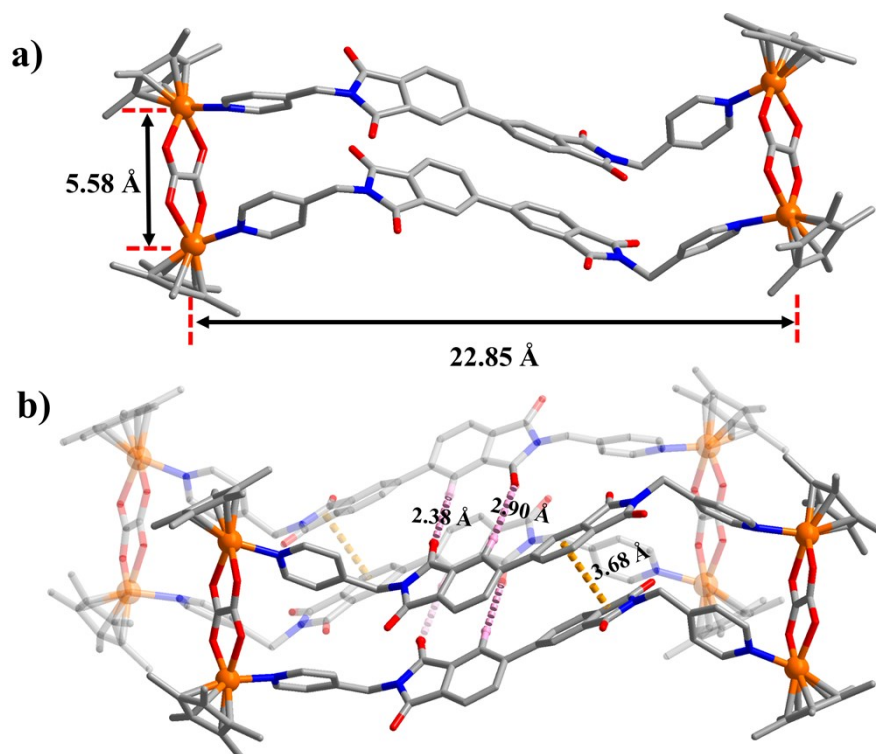


Fig. S3. a) Stick model of **4**; b) Single-crystal X-ray structure of non-interlocked macrocycle **4**; c) π - π stacking (dashed dark yellow lines) and C-H \cdots O hydrogen bond interactions (dashed orange lines) between two macrocycles **4**. Most hydrogen atoms, anions, solvent molecules and disorder are omitted for clarity (N, blue; O, red; C, gray; Rh, violet)

3.4 Single-crystal X-ray structure of **5**

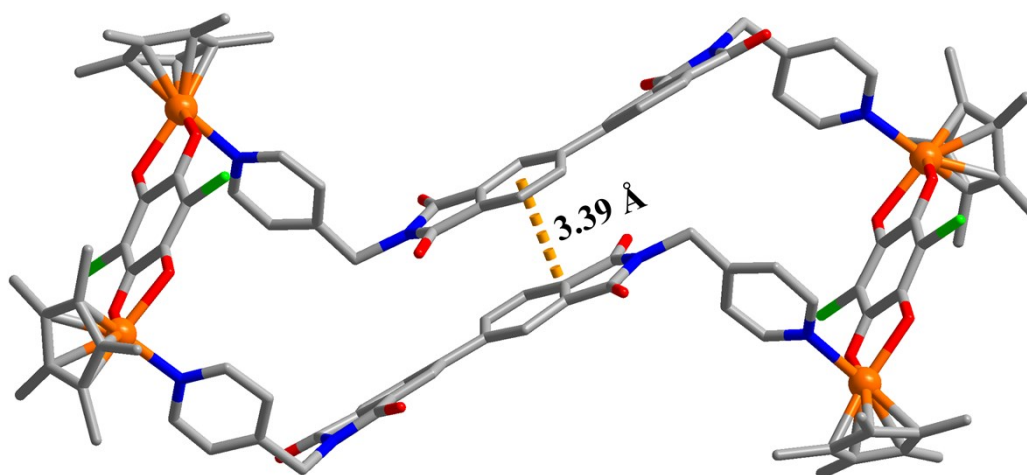


Fig. S4. Single-crystal X-ray structure of **5**. Counteranions and hydrogen atoms are omitted for clarity (N, blue; O, red; C, gray; Rh, orange; Cl, green)

4. NMR Spectra

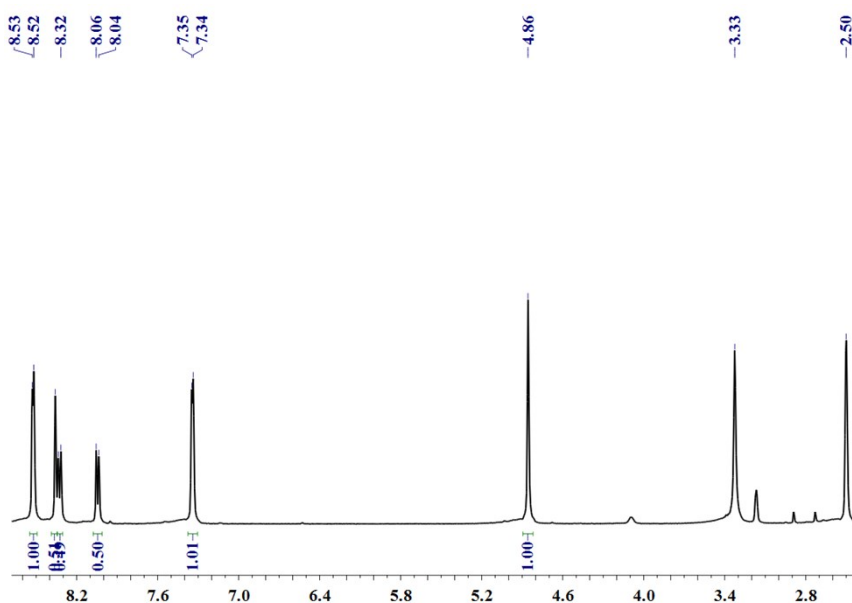


Fig. S5. The ^1H NMR spectra of ligand **L** in DMSO-D6 solution

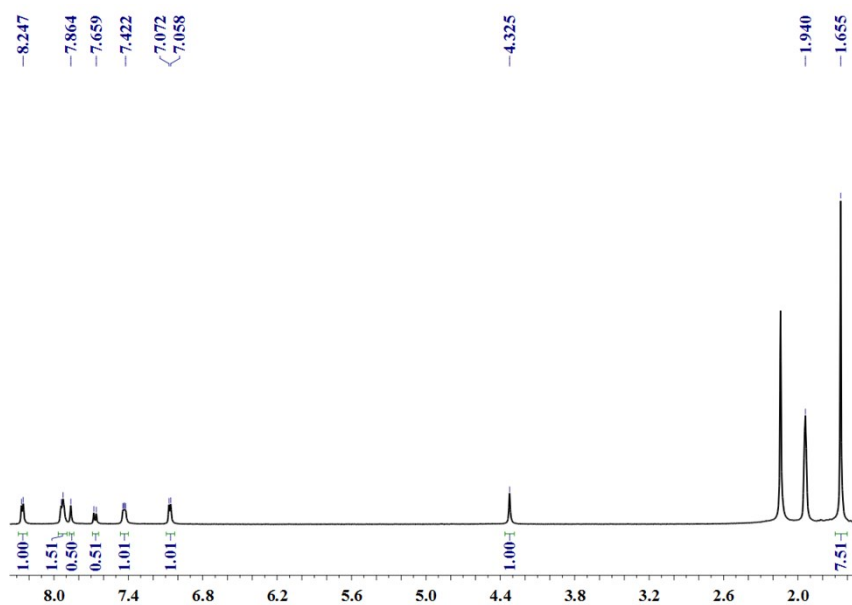


Fig. S6. The ^1H NMR (400 MHz, CD_3CN , ppm) for **1** (12.0 mM, with respect to Cp^*Rh)

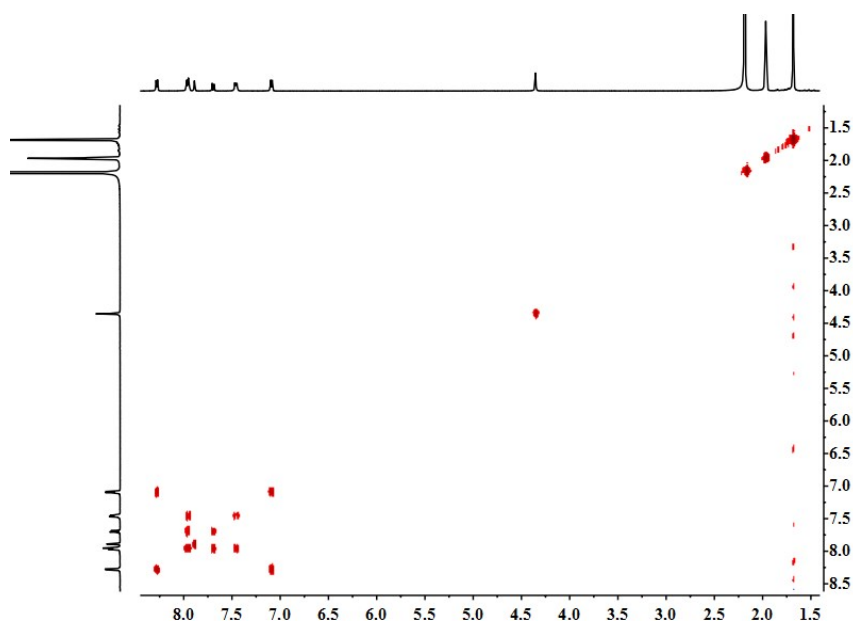


Fig. S7. The ^1H COSY NMR (400 MHz, CD_3CN , ppm) for **1** (12.0 mM, with respect to Cp^*Rh)

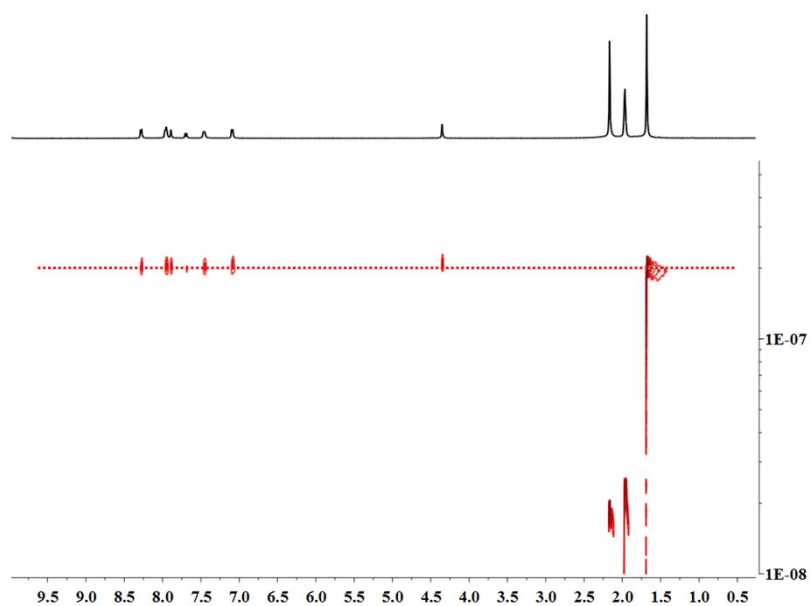


Fig. S8. ^1H DOSY NMR (400 MHz, CD_3CN , ppm) for **1** ($5.04 \times 10^{-10} \text{ m}^2\text{s}^{-1}$) (12.0 mM, with respect to Cp^*Rh)

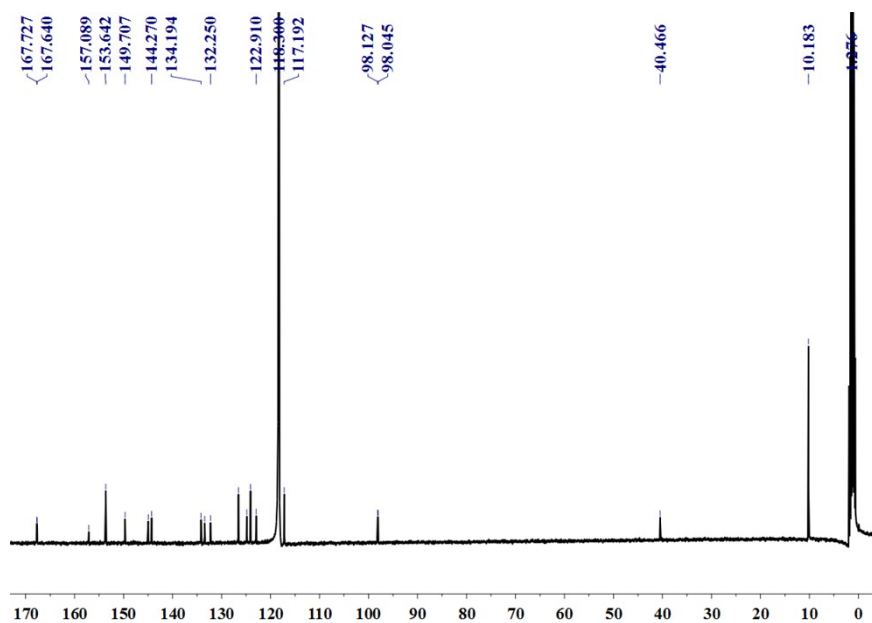


Fig. S9. The $^{13}\text{C}\{^1\text{H}\}$ NMR (101 MHz, CD_3CN , ppm) for **1** (12.0 mM, with respect to Cp^*Rh)

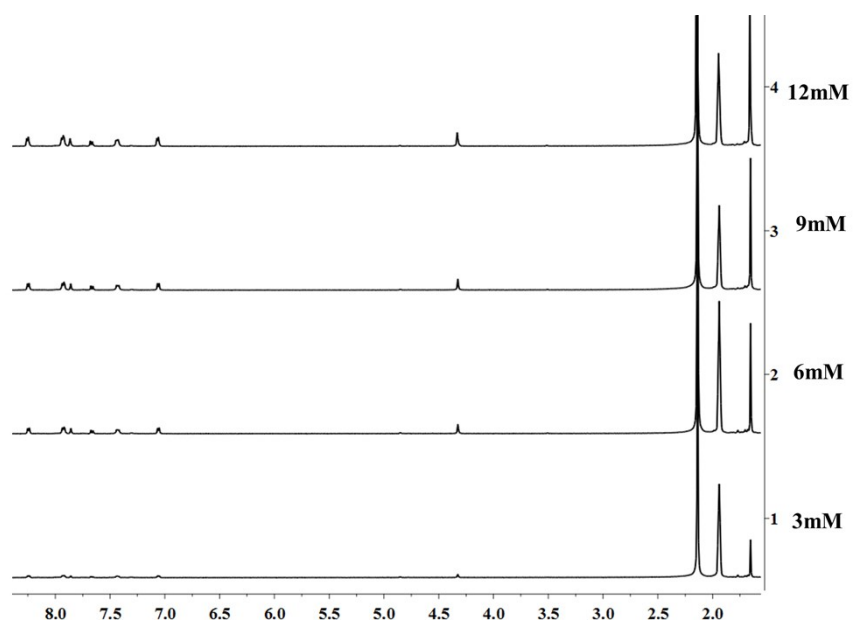


Fig. S10. The ^1H NMR (400 MHz, CD_3CN , ppm) for **1** (3.0 mM to 12.0 mM, with respect to Cp^*Rh)

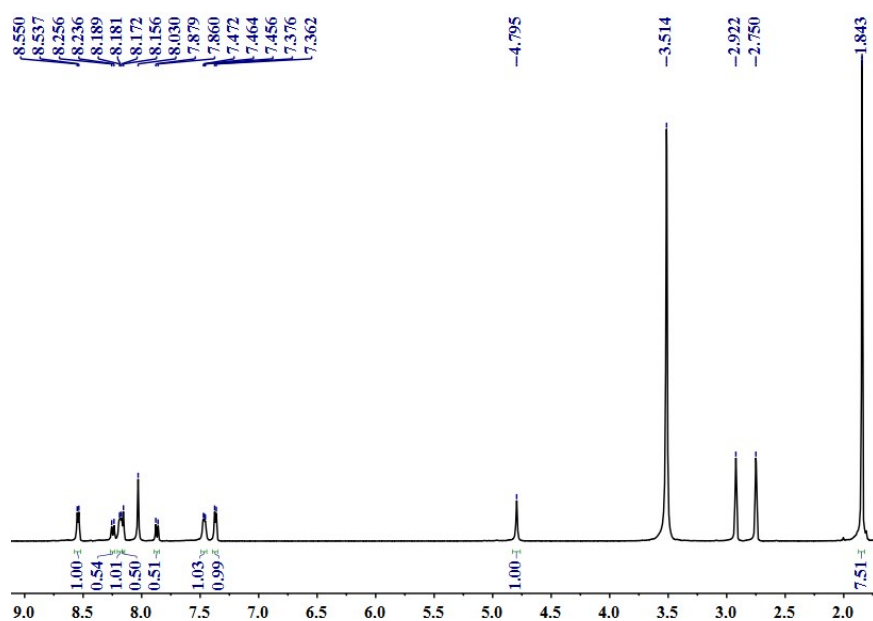


Fig. S11. The ^1H NMR (400 MHz, $[\text{D}_7]$ -DMF, ppm) for **1** (12.0 mM, with respect to Cp^*Rh)

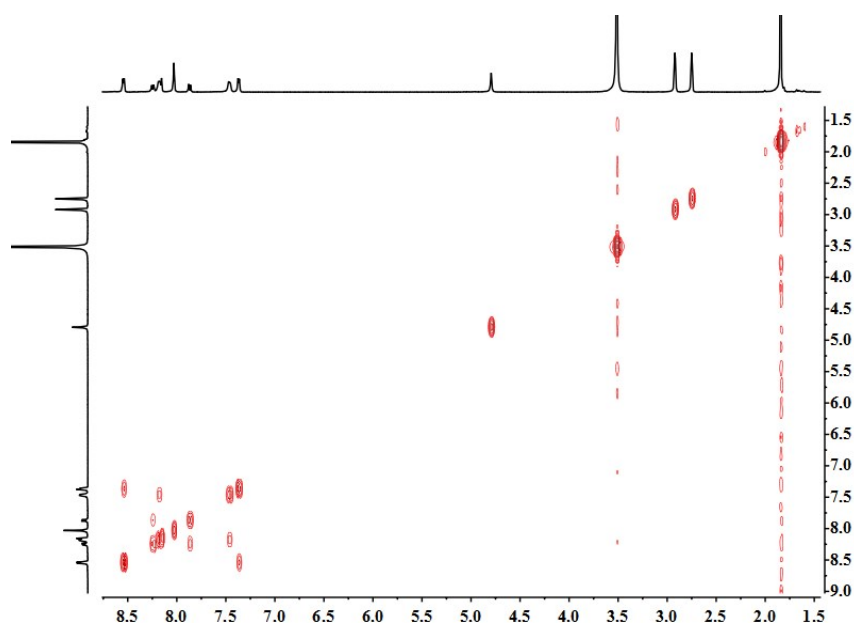


Fig. S12. The ^1H COSY NMR (400 MHz, $[\text{D}_7]$ -DMF, ppm) for **1** (12.0 mM, with respect to Cp^*Rh)

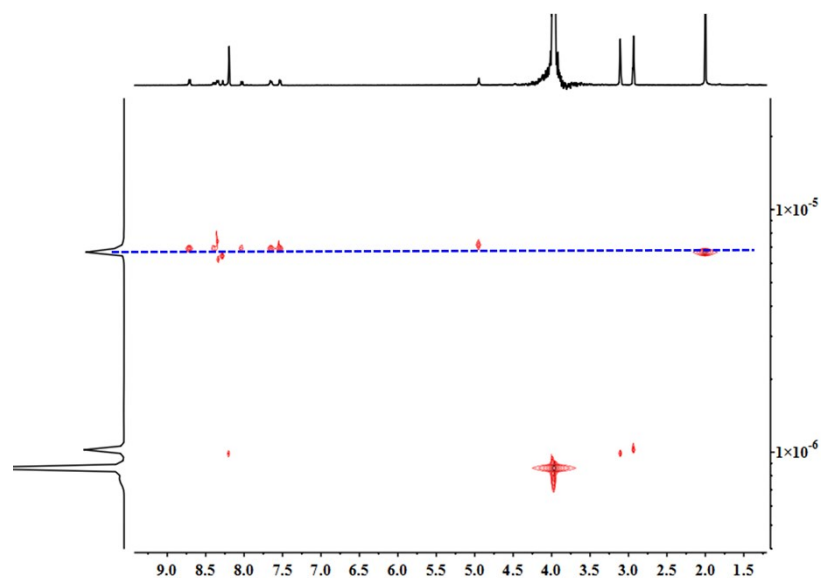


Fig. S13. The ^1H DOSY NMR (400 MHz, $[\text{D}_7]$ -DMF, ppm) for **1** (12.0 mM, with respect to Cp^*Rh) Diffusion coefficient: $1.32 \times 10^{-10} \text{ m}^2\text{s}^{-1}$

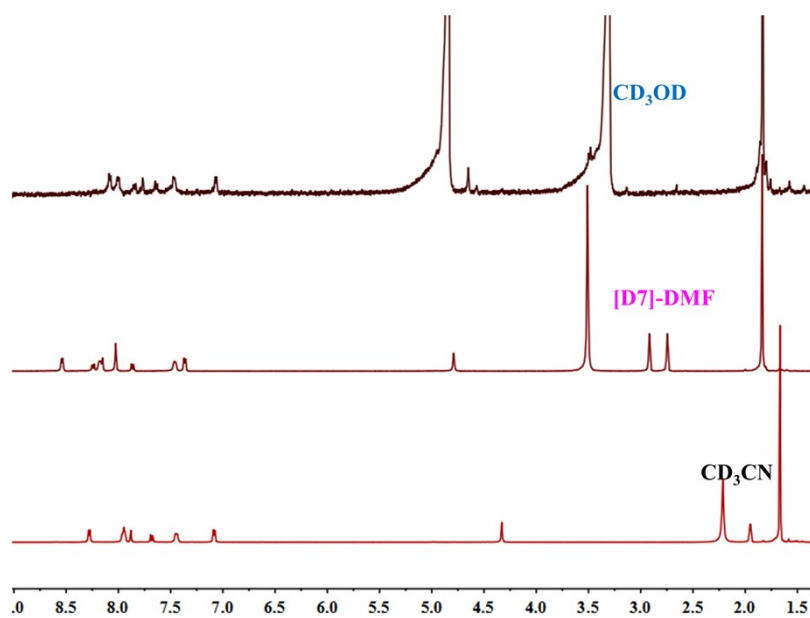


Fig. S14. The comparison ^1H NMR spectra of **1** in CD_3OD , CD_3CN and $[\text{D}_7]$ -DMF solution

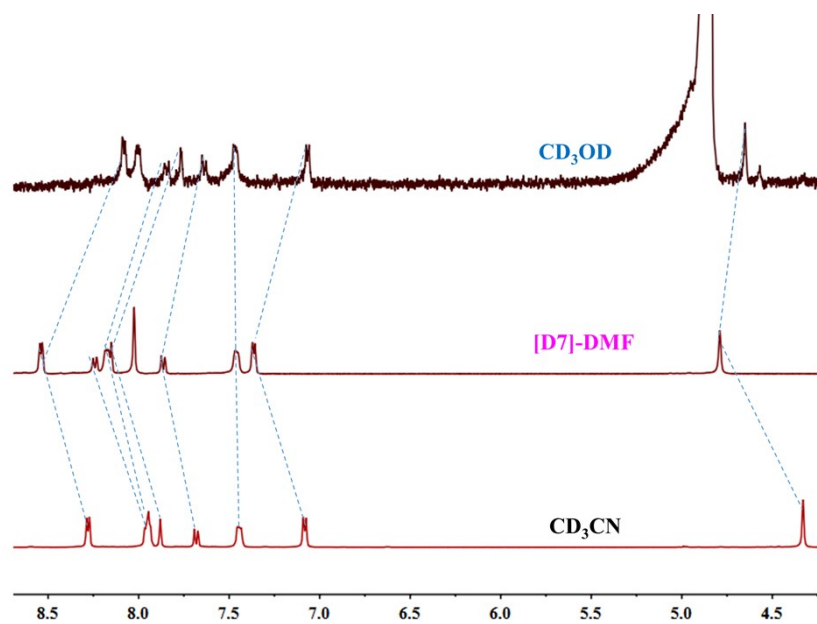


Fig. S15. The partial comparison ^1H NMR spectra of **1** in CD_3OD , CD_3CN and $[\text{D}_7]\text{-DMF}$ solution

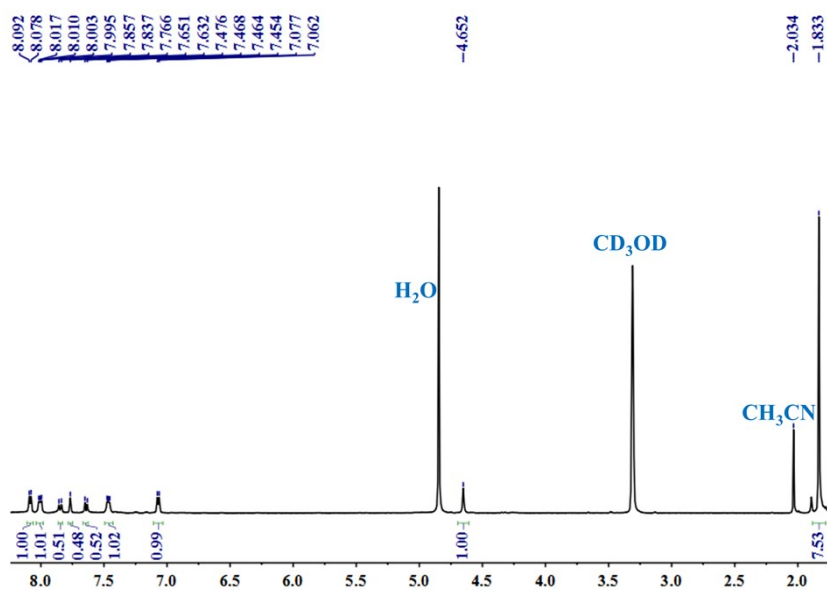


Fig. S16. The ^1H NMR (400 MHz, CD_3OD , ppm) for **1** (8.0 mM, with respect to Cp^*Rh)

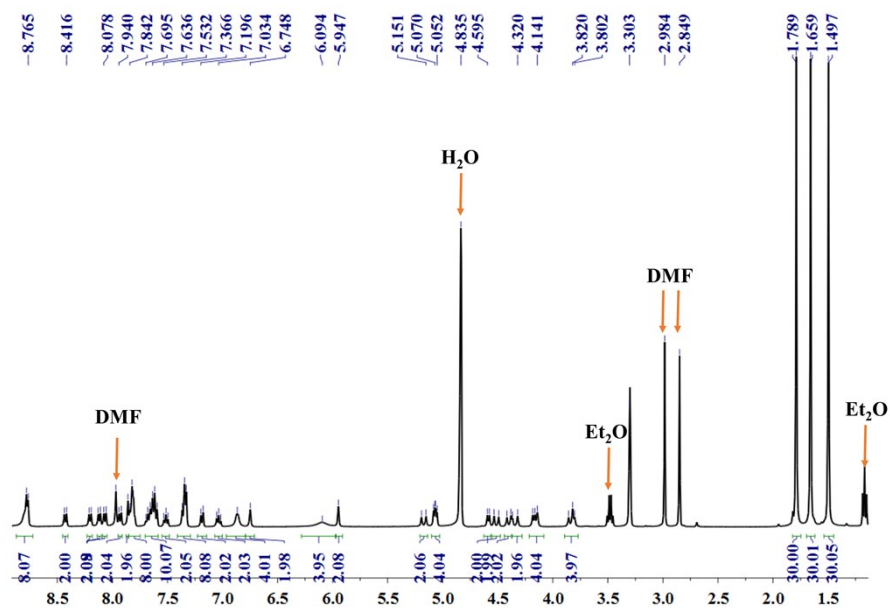


Fig. S17. The ^1H NMR (400 MHz, CD_3OD , ppm) for **3** (20.0 mM, with respect to Cp^*Rh)

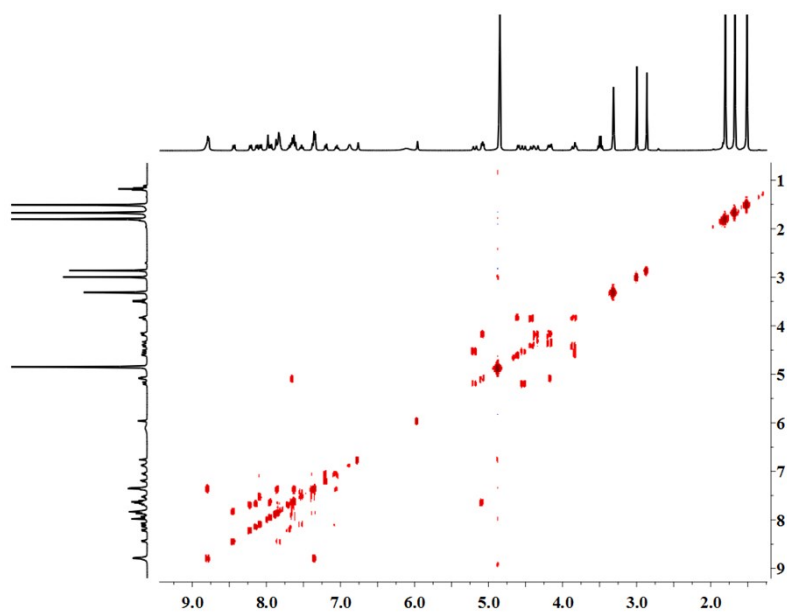


Fig. S18. The ^1H COSY NMR (400 MHz, CD_3OD , ppm) for **3** (20.0 mM, with respect to Cp^*Rh)

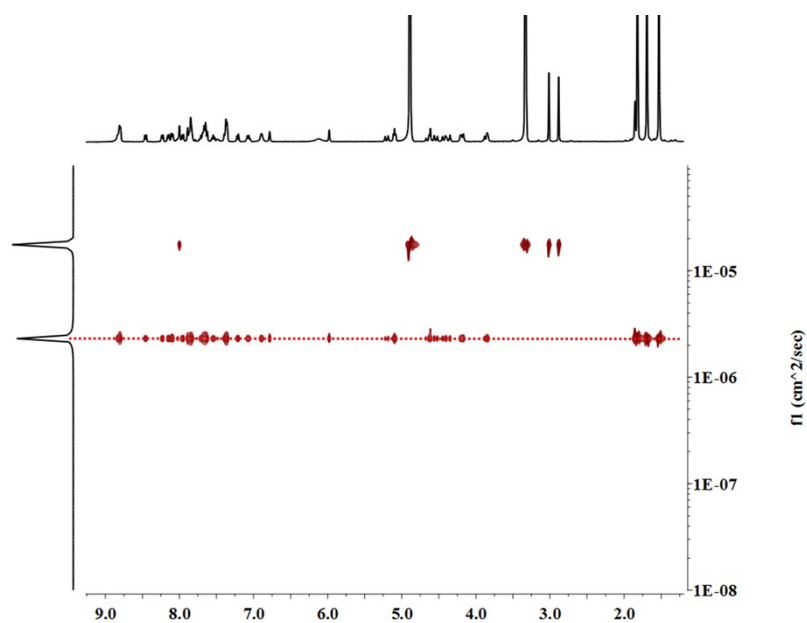


Fig. S19. The ^1H DOSY NMR (400 MHz, CD_3OD , ppm) for **3** (8.0 mM, with respect to Cp^*Rh) Diffusion coefficient: $2.36 \times 10^{-10} \text{ m}^2\text{s}^{-1}$

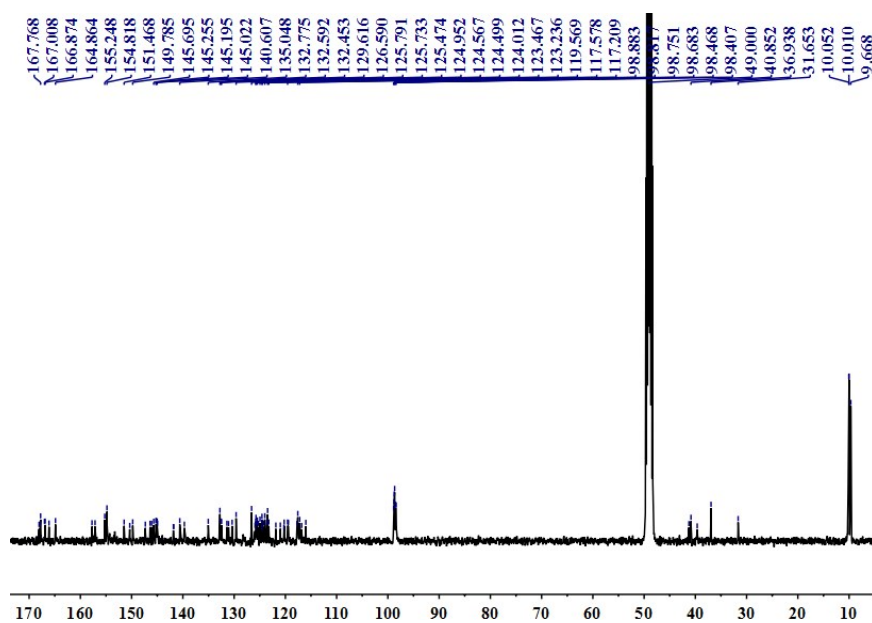


Fig. S20. The $^{13}\text{C}\{^1\text{H}\}$ NMR (101 MHz, CD_3OD , ppm) for **3** (8.0 mM, with respect to Cp^*Rh)

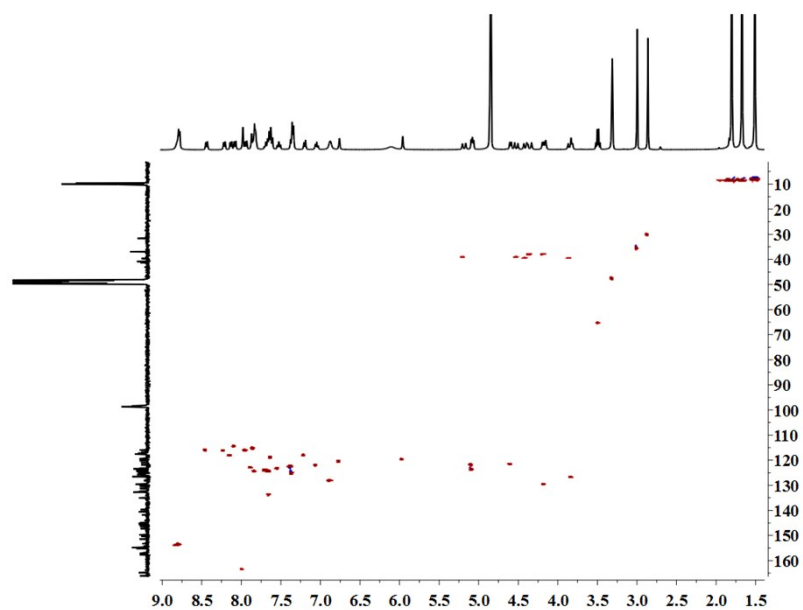


Fig. S21. The ^1H - ^{13}C HSQC NMR (400 MHz, CD_3OD , ppm) for **3** (20.0 mM, with respect to Cp^*Rh)

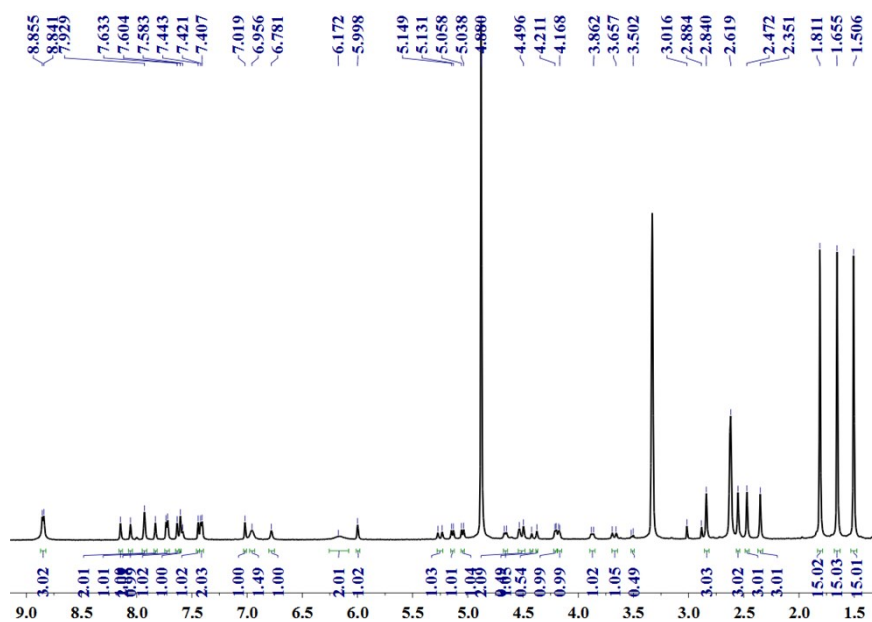


Fig. S22. The ^1H NMR (400 MHz, CD_3OD , ppm) for **3'** (10.0 mM, with respect to Cp^*Rh)

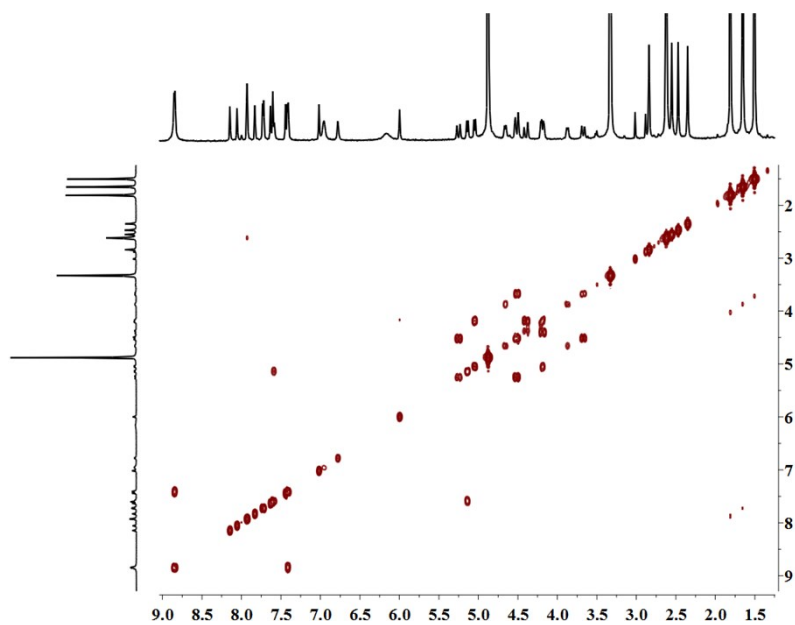


Fig. S23. The ^1H COSY NMR (400 MHz, CD_3OD , ppm) for **3'** (10.0 mM, with respect to Cp^*Rh)

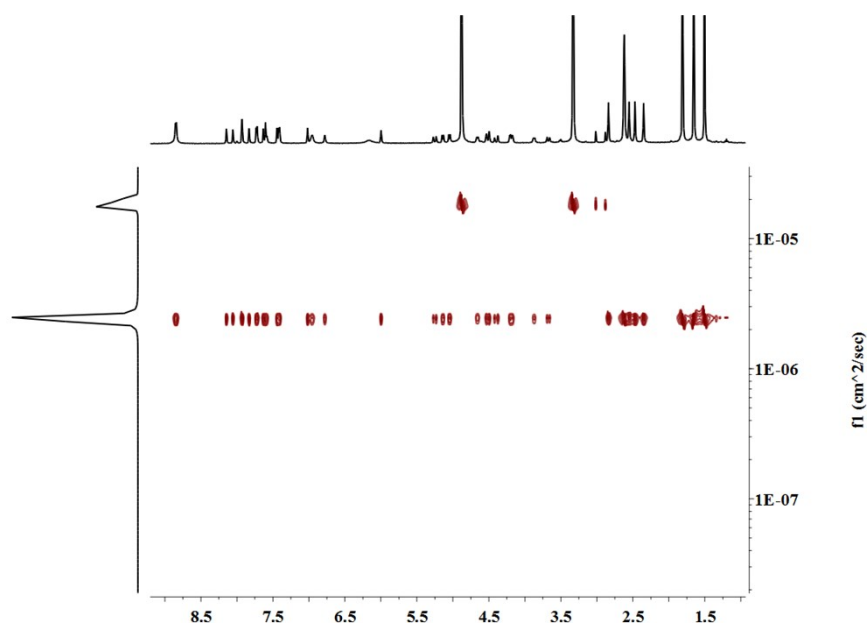


Fig. S24. The ^1H DOSY NMR (400 MHz, CD_3OD , ppm) for **3'** (10.0 mM, with respect to Cp^*Rh) Diffusion coefficient: $2.40 \times 10^{-10} \text{ m}^2\text{s}^{-1}$

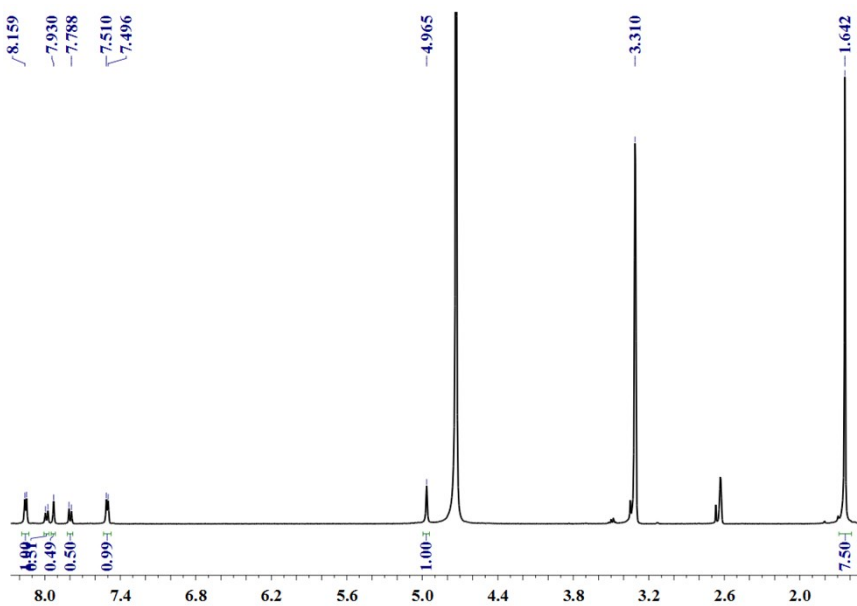


Fig. S25. The ^1H NMR (400 MHz, CD_3OD , ppm) for **4** (10.0 mM, with respect to Cp^*Rh)

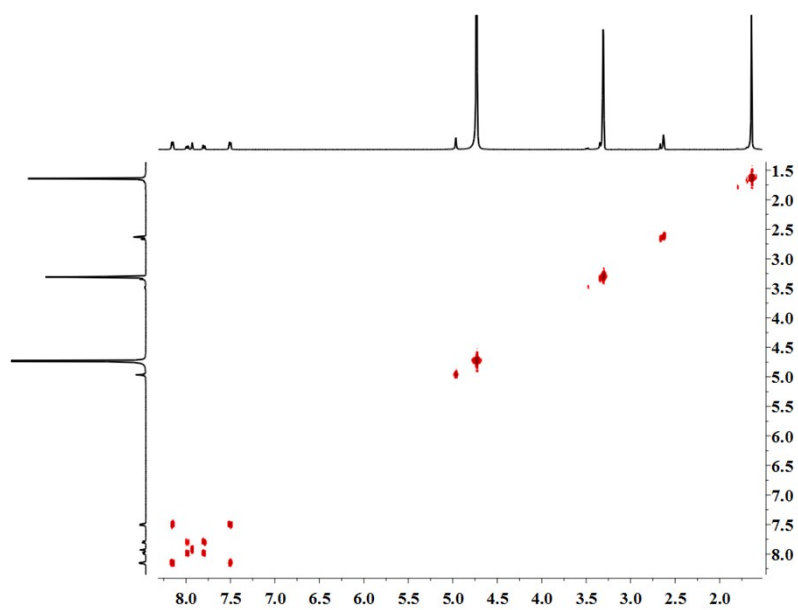


Fig. S26. The ^1H COSY NMR (400 MHz, CD_3OD , ppm) for **4** (10.0 mM, with respect to Cp^*Rh)

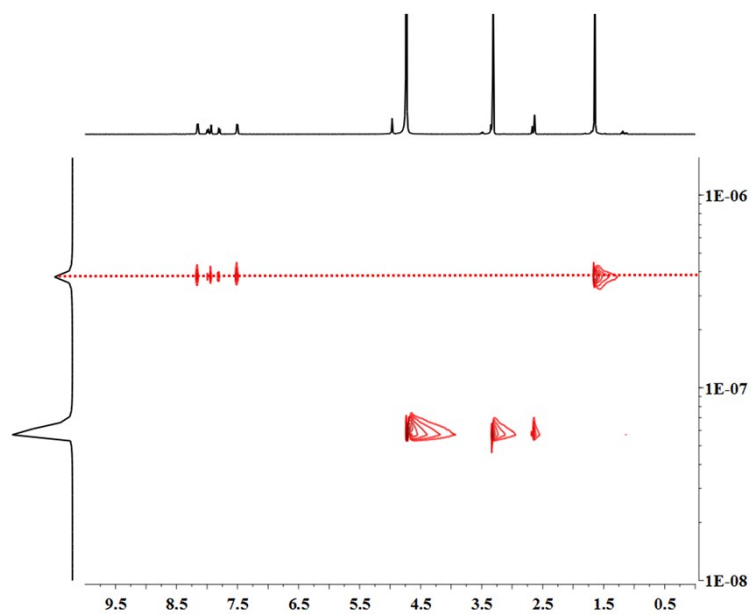


Fig. S27. The ^1H DOSY NMR (400 MHz, CD_3OD , ppm) for **4**. Diffusion coefficient: $2.62 \times 10^{-10} \text{ m}^2\text{s}^{-1}$ (10.0 mM, with respect to Cp^*Rh)

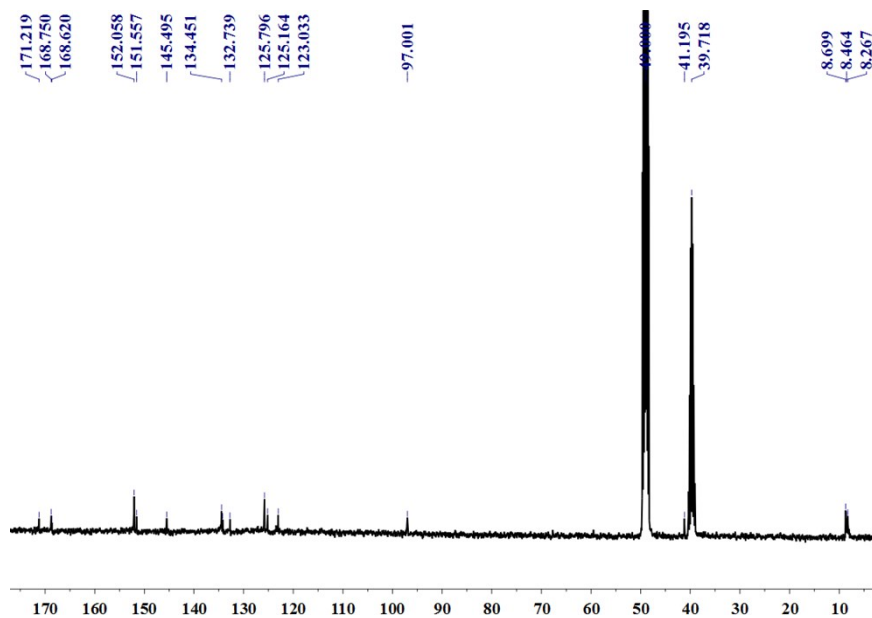


Fig. S28. The $^{13}\text{C}\{^1\text{H}\}$ NMR (101 MHz, CD_3OD , ppm) for **4** (10.0 mM, with respect to Cp^*Rh)

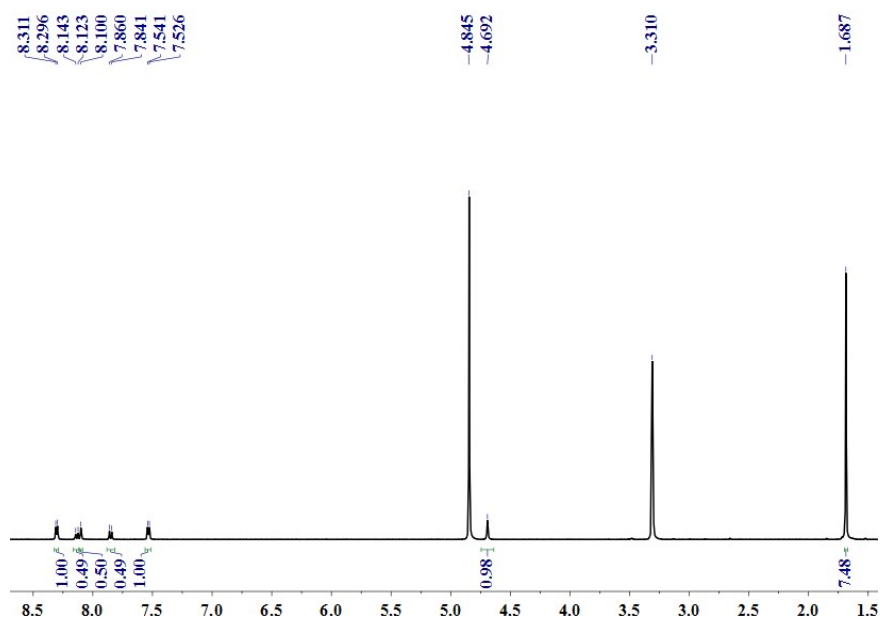


Fig. S29. The ^1H NMR (400 MHz, CD_3OD , ppm) for **5** (15.0 mM, with respect to Cp^*Rh)

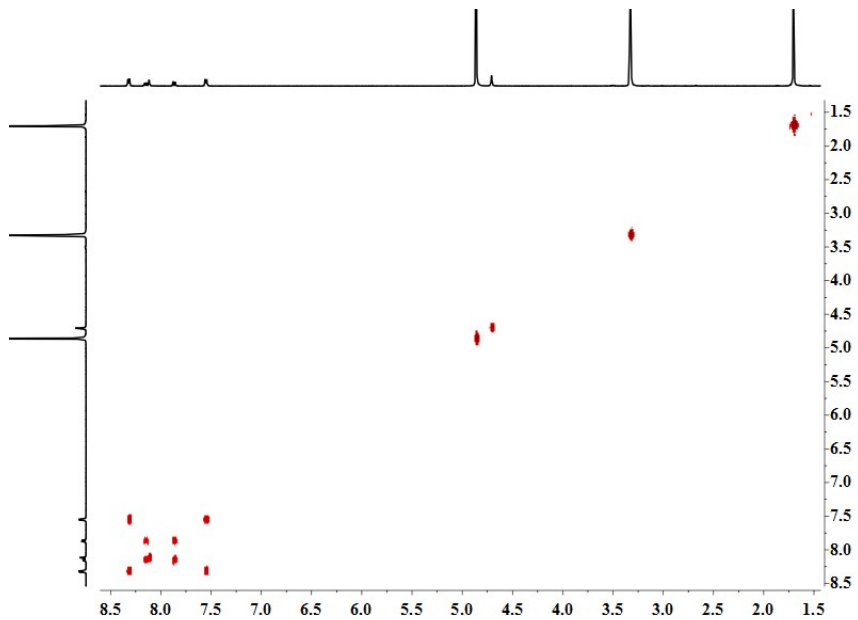


Fig. S30. The ^1H COSY NMR (400 MHz, CD_3OD , ppm) for **5** (15.0 mM, with respect to Cp^*Rh)

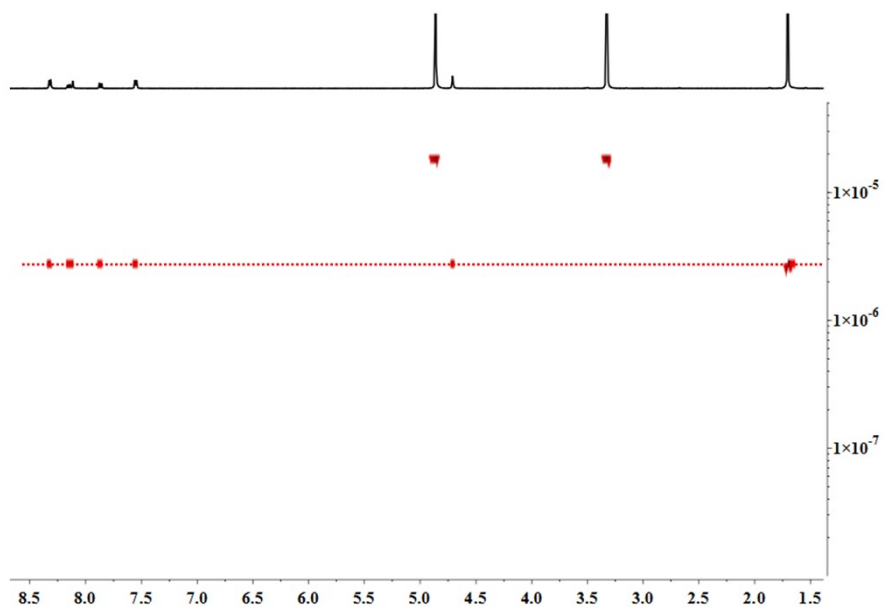


Fig. S31. The ^1H DOSY NMR (400 MHz, CD_3OD , ppm) for **5** (15.0 mM, with respect to Cp^*Rh) Diffusion coefficient: $3.16 \times 10^{-10} \text{ m}^2\text{s}^{-1}$

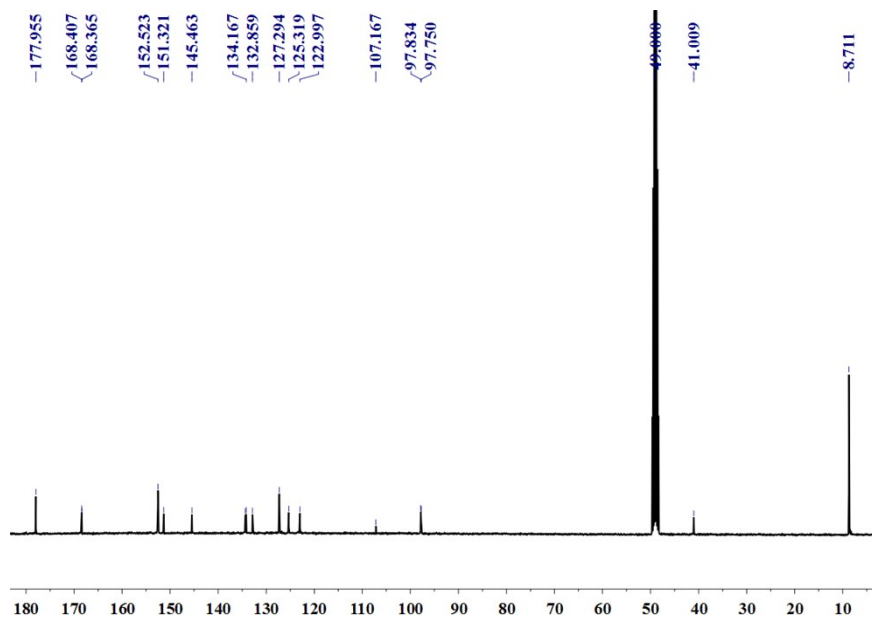


Fig. S32. The $^{13}\text{C}\{^1\text{H}\}$ NMR (101 MHz, CD_3OD , ppm) for complex **5** (15.0 mM, with respect to Cp^*Rh)

5 ESI-MS spectra

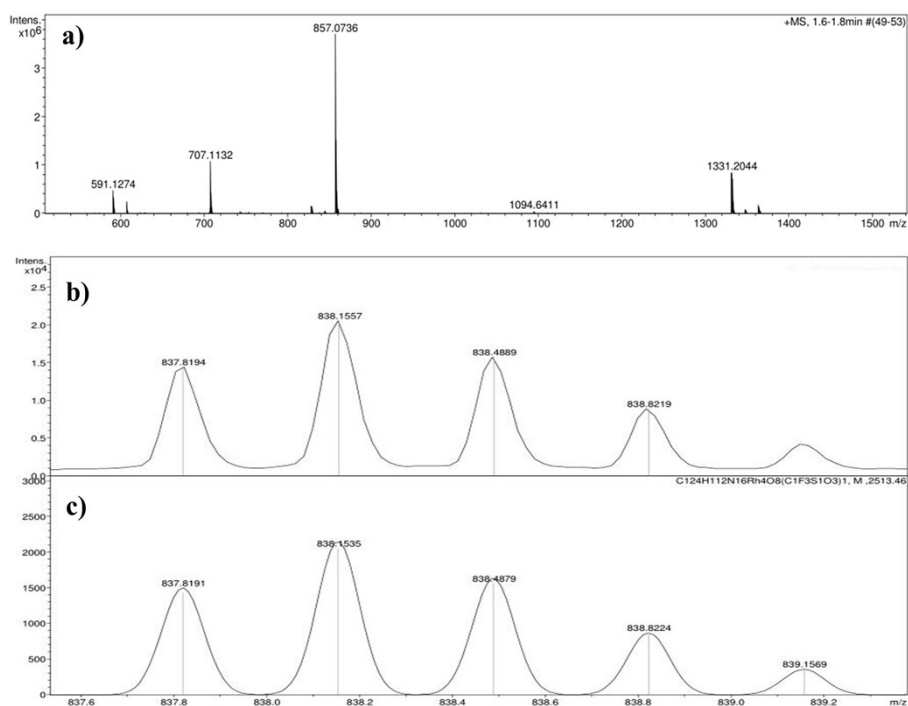


Fig. S33. Full ESI-MS spectra (a) of complex **1**, experimental (b) and theoretical (c) ESI-MS spectra of [1-**3OTf**]³⁺ in CH₃CN solvent

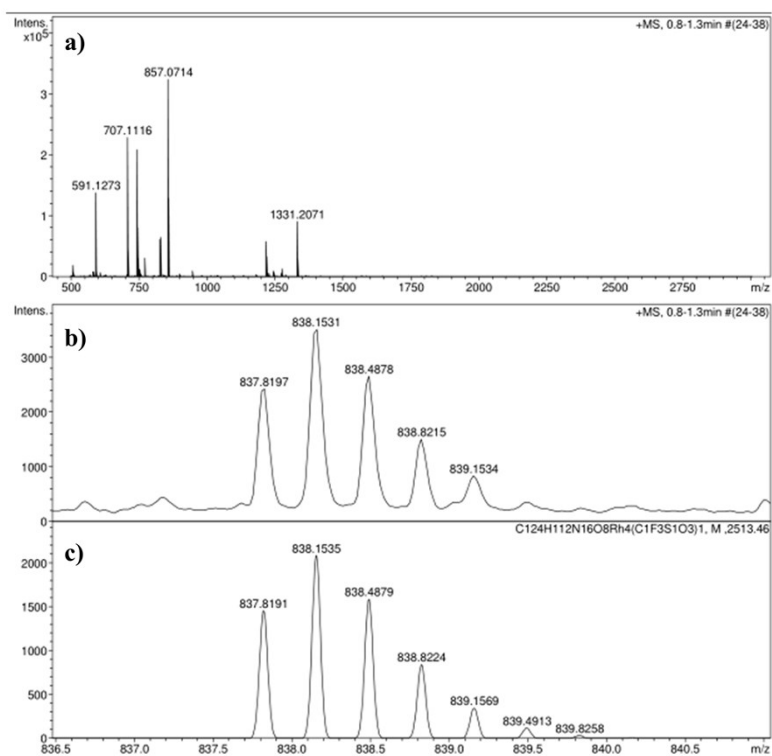


Fig. S34. Full ESI-MS spectra (a) of complex **1**, experimental (b) and theoretical (c) ESI-MS spectra of [1-**3OTf**]³⁺ in DMF solvent

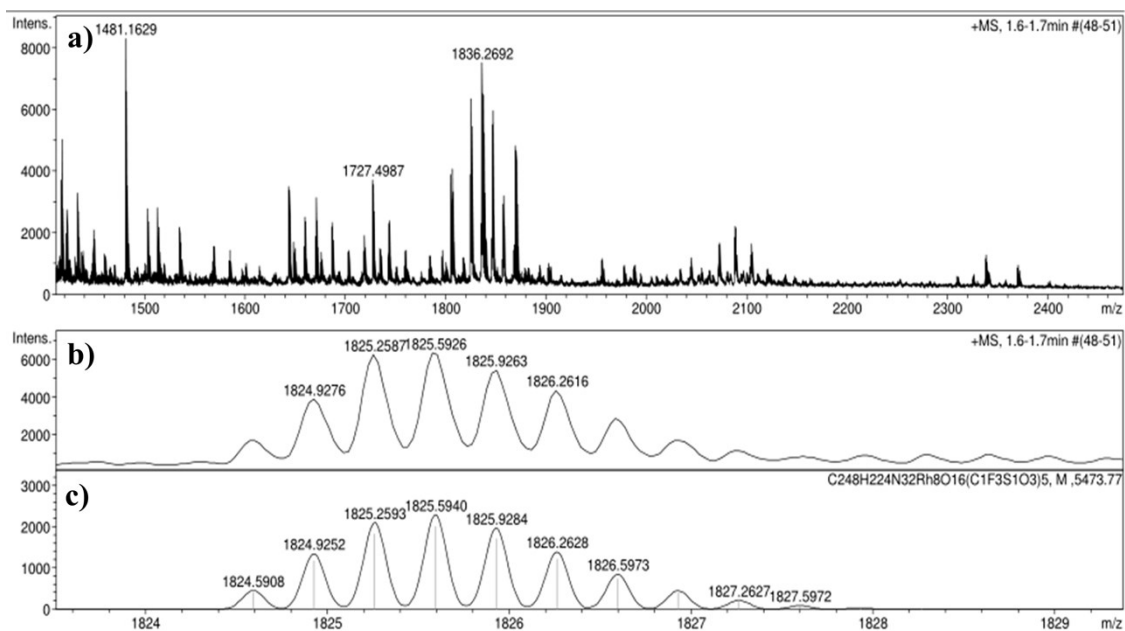


Fig. S35. Full ESI-MS spectra (a) of complex **2**, experimental (b) and theoretical (c) ESI-MS spectra of $[2 - 3OTf]^{3+}$

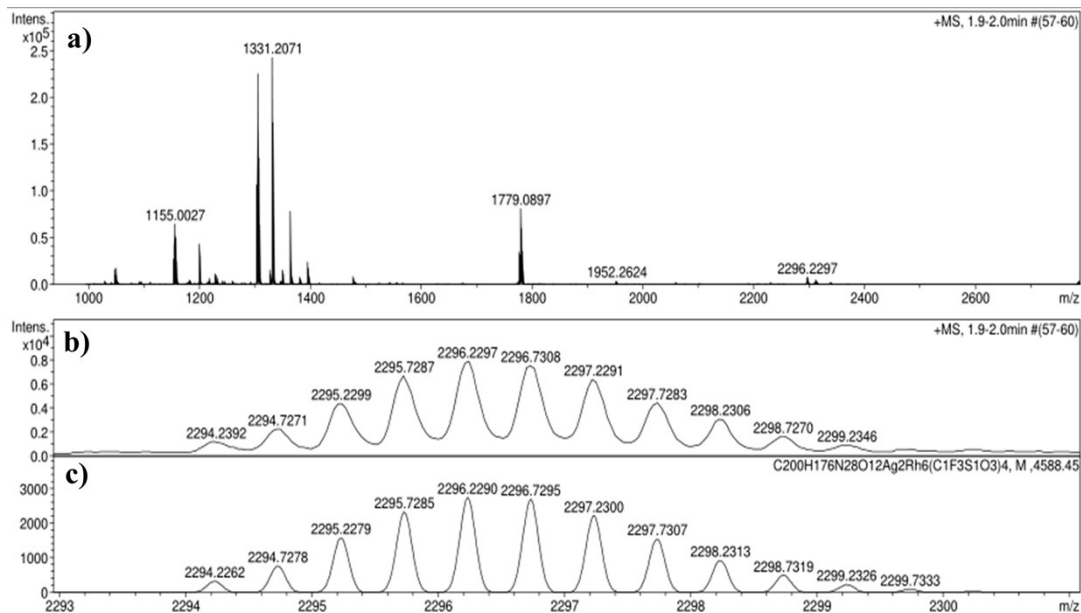


Fig. S36. Full ESI-MS spectra (a) of complex **3**, experimental (b) and theoretical (c) ESI-MS spectra of $[3 - 2OTf]^{2+}$

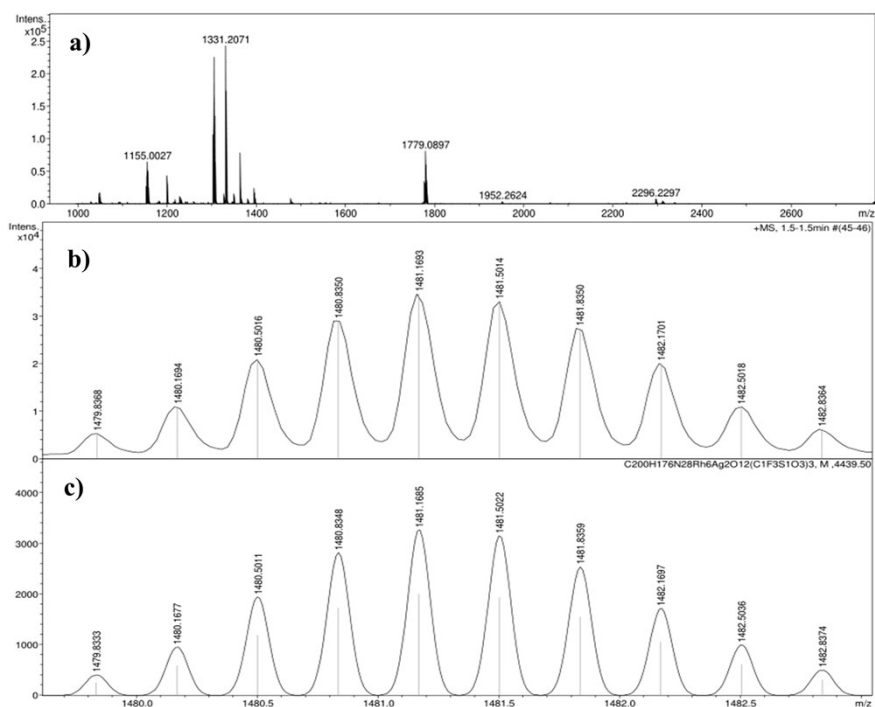


Fig. S37. Full ESI-MS spectra (a) of complex **3**, experimental (b) and theoretical (c) ESI-MS spectra of [**3**-**3OTf**]³⁺

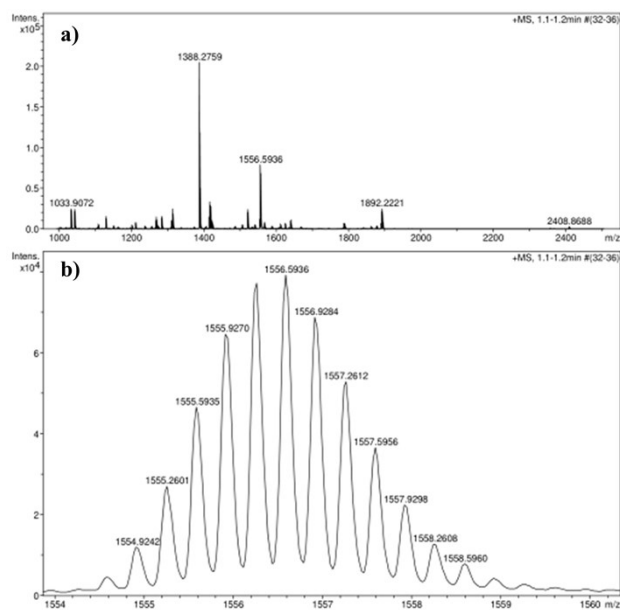


Fig. S38. Full ESI-MS spectra (a) of complex **3'** and experimental (b) ESI-MS spectra of [**3'**-**3OTf**]³⁺

6 X-ray crystallography details

Single crystals of **1'**, **2**, **2'**, **2-pyrene**, **3'** and **4**, suitable for X-ray diffraction study were obtained at room temperature. X-ray intensity data of them were collected at 173 K on a CCD-Bruker SMART APEX system. In these data, the disordered solvent molecules which could not be restrained properly were removed using the SQUEEZE route.

In asymmetric unit of **1'**, there were disordered anion and solvents (one triflate anion, three N,N-dimethylformamide, one methanol and one water molecules) which could not be restrained properly. Therefore, SQUEEZE algorithm was used to omit them. 15 ISOR, 6 DELU and 11 DFIX instructions were used to restrain anion, solvents and Cp* fragments so that there were 108 restraints in the data. Hydrogen of water molecules could not be found and others were put in calculated positions.

In asymmetric unit of **2**, there were disordered solvent molecules (three methanol and eight water molecules) which could not be restrained properly. Therefore, SQUEEZE algorithm was used to omit them. One metallo-angle (Rh4 and coordinated Cp* fragment) and three triflate anions were disordered and they were divided into two parts (34:66 for metallo-angle and 38:62, 69:31, 50:50 for anions). 67 ISOR, 7 SIMU and 30 DFIX instructions were used to restrain anions, ligand and Cp* fragments so that there were 612 restraints in the data. Hydrogen of water molecules could not be found and others were put in calculated positions.

In asymmetric unit of **2'**, there were disordered anions and solvents (three triflate anions, four di-isopropyl ether, four acetonitrile and two water molecules) which could not be restrained properly. Therefore, SQUEEZE algorithm was used to omit them. Three pentamethylcyclopentadienyl ligands (Cp* for short) were disordered and they were divided into two parts (51:49, 59:41 and 60:40). 70 ISOR, 2 SIMU and 4 DFIX instructions were used to restrain anions, ligands and Cp* fragments so that there were 496 restraints in the data.

In asymmetric unit of **2-pyrene**, there were disordered anion and solvents (one triflate anion, four methanol and ten water molecules) which could not be restrained properly. Therefore, SQUEEZE algorithm was used to omit them. One pentamethylcyclopentadienyl ligand (Cp* for short) was disordered and it was divided into two parts (46:54). 62 ISOR, 1 SIMU, 3 DELU and 15 DFIX instructions were used to restrain anions, pyrene molecules and Cp* fragments so that there were 493 restraints in the data.

In asymmetric unit of **3'**, there were disordered anions and solvents (four triflate anions, fourteen diisopropyl ether, five N,N-dimethylformamide, eighteen methanol and sixteen water molecules) which could not be restrained properly. Therefore, SQUEEZE algorithm was used to omit them. One metallo-edge (Rh1, 2, Ag1, 2 and coordinated chelated ligands and Cp* fragments), one metallo-angle (Rh8 and coordinated Cp* fragment), two Cp* fragments and one triflate anion were disordered and they were divided into two parts (55:45 for metallo-edge, 56:44 for metallo-angle, 51:49 and 61:39 for Cp* and 65:35 for anion). F20 and C456 were refined isotropically and other non-hydrogen atoms were refined anisotropically. 228 ISOR, 1 FLAT, 5 SIMU and 70 DFIX instructions were used to restrain anions, ligands, solvents and Cp* fragments so that there were 1764 restraints in the data.

In asymmetric unit of **4**, there were disordered anion and solvents (one triflate anion, two acetonitrile and three water molecules) which could not be restrained properly. Therefore, SQUEEZE algorithm was used to omit them. One triflate anion and one methanol molecule were disordered and they were divided into two parts (52:48 for anion and 63:37 for methanol). 22 ISOR, 1 SIMU and 8 DFIX instructions were used to restrain anions, solvents and Cp* fragments so that there were 206 restraints in the data. Hydrogen of methanol and water molecules could not be found and others were put in calculated positions.

Table 1. Crystal data and structure refinement for 1'

Empirical formula	$C_{154}H_{182}F_{12}Ir_4N_{24}O_{33}S_4$	
Formula weight	4022.27	
Temperature	172.98 K	
Wavelength	1.34138 Å	
Crystal system	Orthorhombic	
Space group	C222 ₁	
Unit cell dimensions	a = 21.4001(8) Å	$\alpha/^\circ = 90^\circ$.
	b = 56.956(2) Å	$\beta/^\circ = 90^\circ$.
	c = 13.5367(4) Å	$\gamma/^\circ = 90^\circ$.
Volume	16499.3(10) Å ³	
Z	4	
Density (calculated)	1.619 Mg/m ³	
Absorption coefficient	5.054 mm ⁻¹	
F(000)	8072	
Crystal size	0.41 x 0.25 x 0.24 mm ³	
Theta range for data collection	3.428 to 58.000°.	
Index ranges	-27<=h<=27, -72<=k<=72, -17<=l<=11	
Reflections collected	61156	
Independent reflections	17437 [R(int) = 0.0524]	
Completeness to theta = 53.594°	99.9 %	
Absorption correction	Semi-empirical from equivalents	
Max. and min. transmission	0.7516 and 0.4410	
Refinement method	Full-matrix least-squares on F ²	
Data / restraints / parameters	17437 / 108 / 819	
Goodness-of-fit on F ²	1.075	
Final R indices [I>2sigma(I)]	R1 = 0.0528, wR2 = 0.1523	
R indices (all data)	R1 = 0.0613, wR2 = 0.1604	
Absolute structure parameter	0.109(17)	
Extinction coefficient	n/a	
Largest diff. peak and hole	2.142 and -0.706 e.Å ⁻³	

Table 2 Crystal data and structure refinement for 2

Empirical formula	$C_{131}H_{146}F_{12}N_{16}O_{34}Rh_4S_4$	
Formula weight	3256.51	
Temperature	173(2) K	
Wavelength	1.34138 Å	
Crystal system	Monoclinic	
Space group	P2 ₁ /n	
Unit cell dimensions	a = 29.994(2) Å	$\alpha/^\circ = 90^\circ$.
	b = 14.8641(8) Å	$\beta/^\circ = 103.709(2)^\circ$
	c = 33.736(2) Å	$\gamma/^\circ = 90^\circ$.
Volume	14612.3(16) Å ³	
Z	4	
Density (calculated)	1.480 Mg/m ³	
Absorption coefficient	3.304 mm ⁻¹	
F(000)	6672	
Crystal size	0.270 x 0.250 x 0.230 mm ³	
Theta range for data collection	3.012 to 55.499°.	
Index ranges	-36<=h<=36, -18<=k<=17, -41<=l<=39	
Reflections collected	103672	
Independent reflections	28218 [R(int) = 0.1004]	
Completeness to theta = 53.594°	99.5 %	
Absorption correction	Semi-empirical from equivalents	
Max. and min. transmission	0.616 and 0.433	
Refinement method	Full-matrix least-squares on F ²	
Data / restraints / parameters	28218 / 612 / 1918	
Goodness-of-fit on F ²	1.036	
Final R indices [I>2sigma(I)]	R1 = 0.0634, wR2 = 0.1650	
R indices (all data)	R1 = 0.0954, wR2 = 0.1883	
Extinction coefficient	n/a	
Largest diff. peak and hole	0.802 and -1.177 e.Å ⁻³	

Table 3. Crystal data and structure refinement for 2-pyrene

Empirical formula	C ₁₅₆ H ₁₆₃ F ₁₂ N ₁₆ O ₃₄ Rh ₄ S ₄	
Formula weight	3573.89	
Temperature	173(2) K	
Wavelength	1.34138 Å	
Crystal system	Triclinic	
Space group	P-1	
Unit cell dimensions	a = 14.7048(6) Å	$\alpha/^\circ = 105.589(2)^\circ$.
	b = 20.1231(9) Å	$\beta/^\circ = 95.648(2)^\circ$.
	c = 28.5603(12) Å	$\gamma/^\circ = 100.981(2)^\circ$.
Volume	7890.6(6) Å ³	
Z	2	
Density (calculated)	1.504 Mg/m ³	
Absorption coefficient	3.096 mm ⁻¹	
F(000)	3670	
Crystal size	0.750 x 0.620 x 0.370 mm ³	
Theta range for data collection	3.233 to 54.924°.	
Index ranges	-17<=h<=17, -24<=k<=24, -34<=l<=34	
Reflections collected	99482	
Independent reflections	29929 [R(int) = 0.0734]	
Completeness to theta = 53.594°	99.8 %	
Absorption correction	Semi-empirical from equivalents	
Max. and min. transmission	0.751 and 0.498	
Refinement method	Full-matrix least-squares on F ²	
Data / restraints / parameters	29929 / 493 / 1863	
Goodness-of-fit on F ²	1.030	
Final R indices [I>2sigma(I)]	R1 = 0.0666, wR2 = 0.1810	
R indices (all data)	R1 = 0.0958, wR2 = 0.2024	
Extinction coefficient	n/a	
Largest diff. peak and hole	1.195 and -1.269 e.Å ⁻³	

Table 4. Crystal data and structure refinement for 2'

Empirical formula	$C_{160}H_{184}F_{12}Ir_4N_{20}O_{26}S_4$	
Formula weight	3928.30	
Temperature	173(2) K	
Wavelength	1.34138 Å	
Crystal system	Monoclinic	
Space group	P2 ₁ /n	
Unit cell dimensions	a = 30.1831(13) Å	$\alpha/^\circ = 90^\circ$.
	b = 15.0508(8) Å	$\beta/^\circ = 103.152(2)^\circ$
	c = 33.4363(15) Å	$\gamma/^\circ = 90^\circ$.
Volume	14791.0(12) Å ³	
Z	4	
Density (calculated)	1.764 Mg/m ³	
Absorption coefficient	5.389 mm ⁻¹	
F(000)	7888	
Crystal size	0.150 x 0.114 x 0.062 mm ³	
Theta range for data collection	3.215 to 56.997°.	
Index ranges	-37<=h<=37, -18<=k<=18, -41<=l<=40	
Reflections collected	108399	
Independent reflections	30170 [R(int) = 0.0795]	
Completeness to theta = 53.594°	99.7 %	
Absorption correction	Semi-empirical from equivalents	
Max. and min. transmission	0.751 and 0.475	
Refinement method	Full-matrix least-squares on F ²	
Data / restraints / parameters	30170 / 496 / 1644	
Goodness-of-fit on F ²	1.033	
Final R indices [I>2sigma(I)]	R1 = 0.0704, wR2 = 0.2096	
R indices (all data)	R1 = 0.0909, wR2 = 0.2274	
Extinction coefficient	n/a	
Largest diff. peak and hole	2.284 and -2.188 e.Å ⁻³	

Table 5. Crystal data and structure refinement for 3'

Empirical formula	$C_{286}H_{393}Ag_2F_{18}N_{31}O_{58}Rh_6S_6$	
Formula weight	6560.85	
Temperature	173.0 K	
Wavelength	1.34138 Å	
Crystal system	Monoclinic	
Space group	P121/c1	
Unit cell dimensions	$a = 36.050(2)$ Å	$\alpha/^\circ = 90^\circ$
	$b = 39.906(2)$ Å	$\beta/^\circ = 108.546(2)^\circ$
	$c = 43.383(2)$ Å	$\gamma/^\circ = 90^\circ$
Volume	$59170(6)$ Å ³	
Z	8	
Density (calculated)	1.473 Mg/m ³	
Absorption coefficient	3.209 mm ⁻¹	
F(000)	27296	
Crystal size	0.114 x 0.067 x 0.054 mm ³	
Theta range for data collection	2.883 to 53.499°.	
Index ranges	-43<=h<=43, -47<=k<=43, -51<=l<=49	
Reflections collected	417040	
Independent reflections	106410 [R(int) = 0.0549]	
Completeness to theta = 53.499°	99.8 %	
Absorption correction	Semi-empirical from equivalents	
Max. and min. transmission	0.7506 and 0.3223	
Refinement method	Full-matrix least-squares on F ²	
Data / restraints / parameters	106410 / 1764 / 4506	
Goodness-of-fit on F ²	1.052	
Final R indices [I>2sigma(I)]	R1 = 0.0986, wR2 = 0.2611	
R indices (all data)	R1 = 0.1085, wR2 = 0.2668	
Extinction coefficient	n/a	
Largest diff. peak and hole	1.520 and -1.576 e.Å ⁻³	

Table 6 Crystal data and structure refinement for 4

Empirical formula	$C_{109}H_{114}F_{12}N_{10}O_{33}Rh_4S_4$	
Formula weight	2859.98	
Temperature	173(2) K	
Wavelength	1.34138 Å	
Crystal system	Triclinic	
Space group	P-1	
Unit cell dimensions	$a = 15.7031(6)$ Å	$a = 83.5480(10)^\circ$.
	$b = 15.8728(6)$ Å	$b = 76.3810(10)^\circ$.
	$c = 27.7808(10)$ Å	$g = 62.2900(10)^\circ$.
Volume	$5957.9(4)$ Å ³	
Z	2	
Density (calculated)	1.594 Mg/m ³	
Absorption coefficient	3.928 mm ⁻¹	
F(000)	2908	
Crystal size	0.120 x 0.060 x 0.050 mm ³	
Theta range for data collection	2.736 to 53.998°.	
Index ranges	-17<=h<=18, -19<=k<=19, -33<=l<=33	
Reflections collected	65345	
Independent reflections	21799 [R(int) = 0.1159]	
Completeness to theta = 53.594°	99.6 %	
Absorption correction	Semi-empirical from equivalents	
Max. and min. transmission	0.616 and 0.433	
Refinement method	Full-matrix least-squares on F ²	
Data / restraints / parameters	21799 / 206 / 1499	
Goodness-of-fit on F ²	1.000	
Final R indices [I>2sigma(I)]	R1 = 0.0751, wR2 = 0.1934	
R indices (all data)	R1 = 0.0957, wR2 = 0.2087	
Extinction coefficient	n/a	
Largest diff. peak and hole	2.230 and -1.540 e.Å ⁻³	

7 References

1. C. White, A. Yates and P. M. Maitlis, η^5 -Pentamethylcyclopentadienyl) rhodium and -iridium compounds. *Inorg. Synth.*, **1992**, *29*, 228–234.
2. T. Wu, L. H. Weng and G. X. Jin, Sunlight induced cycloaddition and host–guest property of self-assembled organometallic macrocycles based on a versatile building block. *Chem. Comm.*, **2012**, *48*, 4435–4437.
3. E. Muller, G. Bernardinelli, J. Reedijk, 4, 4'-Bis (2-picolimino)-2,2'-bibenzimidazoles: A New Class of Dinucleating Ligands Which Allow for a Tuning of the Metal-Metal Distance. Structures and Properties of a Dicopper (II) Complex and of Two Oxygenation Products of a Dicopper(I) Complex: A Tentative Coordination Chemical Modeling of Hemocyanin. *Inorg. Chem.*, **1995**, *34*, 5979–5988.
4. Y.-F. Han, Y.-J. Lin, W.-G. Jia, L.-H. Weng and G.-X. Jin, Stepwise Formation of Tetra- and Hexanuclear Iridium and Rhodium Complexes Containing Oxalato Ligands. *Organometallics*, **2007**, *26*, 5848-5853.
5. B. B. Guo, Y. J. Lin, G.-X. Jin, Design of and Stability Studies on Trefoil Knots Featuring Cp*Rh Building Blocks. *Chem. Eur. J.* **2019**, *25*, 9721–9727.
6. Y.-F. Han, H. Li, Z.-F. Zheng and G.-X. Jin, Self-Assembled Hexanuclear Organometallic Cages: Synthesis, Characterization, and Host-Guest Properties. *Chem. – Asian J.*, **2012**, *7*, 1243-1250.
7. Q.-X. Cheng, J.-J. Lan, Y.-Q. Chen, J. Lin, R. C. K. Reddy, X. M.-Lin, Y.-P. Cai, 1D helical silver(I)-based coordination polymer containing pyridyl diimide ligand for Fe(III) ions detection. *Inorg. Chem. Commun.*, **2018**, *96*, 30–33.